Fatigue Analysis of Semi-submersible

Yeoh Gim Kok

Master Thesis

presented in partial fulfillment
of the requirements for the double degree:
“Advanced Master in Naval Architecture” conferred by University of Liege
"Master of Sciences in Applied Mechanics, specialization in Hydrodynamics, Energetics and Propulsion” conferred by Ecole Centrale de Nantes

developed at West Pomeranian University of Technology, Szczecin
in the framework of the

Supervisor: Prof. Maciej Taczała, West Pomeranian University of Technology, Szczecin.

Reviewer: Prof. Hervé Le Sourne, L'Institut Catholique d'Arts et Métiers, Nantes.

Szczecin,January 2017

ABSTRACT

Semi-submersible rig is widely used in offshore oil and gas industry, mostly for drilling, exploration and accommodation purpose. It can be operated in deep waters and harsh environments. In comparison to Jack-Up rigs using in shallower waters, semi-submersible rigs are with higher payload capacity and deck area. The design of semi-submersible has evolved much since the very first generation and for this report, a braceless ring pontoon semi-submersible with four columns are studied. Some modules from Sesam, a software suite developed by DNV-GL are used to perform the analyses. Finite element models are prepared based on technical drawings with some reasonable simplification and hydrodynamic analyses are performed to estimate the global responses of the structure. The global responses of the unit in terms of motion and loads are studied.

By using charts and graphs available in the documents of classification societies as a reference, a quick screen is performed to find out the allowable stress range and then together with the results of hydrodynamic analyses, the critical locations with stresses higher than the allowable stress range that need further analyses such as the connection points between pontoons and columns are selected. Stochastic fatigue analyses are then performed to estimate the fatigue life and usage factor of the location concerned.

In addition, the existing semi-submersible is compared with the original design without sponsons added on columns to check the possible impacts of sponsons in motion, hydrodynamic load distribution and fatigue life.

NOMENCLATURE

σ_n	Nominal stress
σ_{max} & σ_{min}	Maximum & minimum stress
σ_{hs}	Hot spot stress
K_g & K_w	Stress concentration factor
σ_p	Notch stress
k	Weibull scale
h	Weibull shape
N_R	Number of stress cycles
A_{33}	Added mass
T_3	Heave period
C_A	Added mass coefficient
C_D	Drag Coefficient
k	Spring stiffness
A_w	Waterplane area

FEA	Finite Element Analysis
FE	Finite Element
SCR	Stress Concentration Factor
RAO	Response Amplitude Operator

CONTENTS

List of Figures

List of Tables

1 INTRODUCTION

1.1 Background

Before the oil price plunged from its peak in 2014, the growing demand for affordable and reliable energy especially fossil fuels has driven oil companies to invest in deep water exploration and drilling in order to tap the deep water reserves. With technological advances, reserves in deep or ultra-deep water are now more accessible with drilling rigs that are specially designed for the water depth like semi-submersibles and drillships. Drillships are with good mobility, higher payload and capable of holding more equipment onboard and semi-submersibles are with high payload and better stability with in terms of lesser rolling and pitching during drilling operations. In addition, global warming makes the Arctic and other icy regions more accessible for oil companies to carry out exploration and drilling in order to tap the possibly massive oil reserve in the region. Specially designed semi-submersibles and drillships that are able to work in arctic conditions seem to be attractive and practicable options for the possible massive oil and gas development in arctic region.

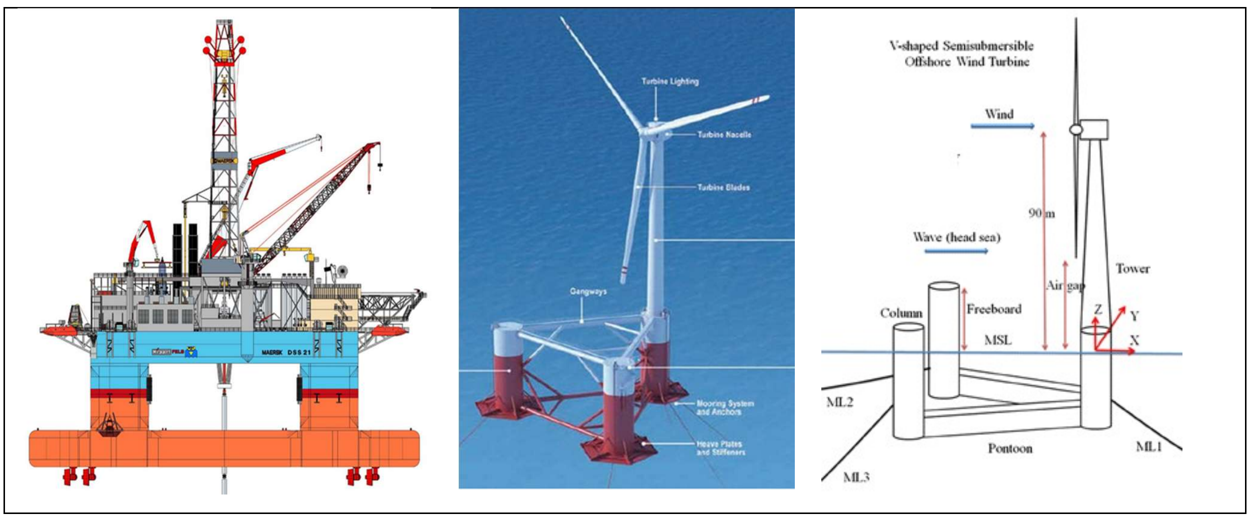

Figure 1 Semi-Submersible for Oil and Gas industries (Left) **[1]**; for wind energy industry (mid & right) **[2] [3]**

In Europe, wind power, either onshore or offshore, is typically used to decrease reliance on fossil fuels and reduce the carbon emission. The first offshore windfarm is installed in Denmark since 1991 and the largest wind offshore wind farm is located in United Kingdom with capacity of 630MW. There is an increasing number of offshore wind turbine structures designed and tested especially for deep water, as a replacement to monopole or other types of bottom fixed support structure foundation that are commonly used at shallow water. These structures are usually in the forms of spar buoy, tensioned leg platform or semi-submersible and the structures need to provide a stable foundation to the wind turbine mounted on top and stand the environmental loadings of wind and waves. One of the most common offshore wind semisubmersible designs is WindFloat, as shown in **Figure 1**. Some slender braces are used to connect the columns of semi-submersible together. The hydro-aerodynamic loads generated by the wind turbine on the top are transferred to the braces and thus cause stress concentration in the welded connections that may leads to possible fatigue damage in long term. In order to avoid the aforementioned problem, the columns of semi-submersible are connected by large dimensioned pontoons without the existence of any kinds of braces such as the V-shape semi-submersible shown in **Figure 1**.

This thesis focuses on the fatigue problem of semi-submersible structure which is used widely in offshore and possibly in wind power industry in future. Fatigue is one of the unavoidable problems for offshore steel structure. Depend on the design, a semi-submersible hull structure consists of connections that are susceptible to fatigue damage. Fatigue analyses should be performed during design stage to ensure that the hull structure is with an adequate fatigue life. In addition, regular maintenance, carefully planned inspection and repairs are required from time to time to ensure the safety and operability of the floating structure during its design life.

1.2 Semi-submersible

A semi-submersible is a type of floating structure designed to operate in deep water and harsh environment. The semi-submersible discussed here is the typical used for offshore industry for drilling, exploration and other purposes. The structure usually consists of a twin-hull or a ring pontoon structure that supports four, six or more columns extending vertically from the pontoons above the operating drafts. A superstructure deck or a box–typed structure is located on the top of the columns.

A typical semi-submersible is usually with at least two operating drafts. And depend on the stage of a project the rig involved in, it can be in transit condition in which the structure is afloat on the pontoon or operating condition when the structure is semi-submerged with sea level higher than the pontoons. The buoyancy needed is mainly obtained from the ballasted pontoons and partially from columns. For some converted and modified semi-submersibles, sponsons and blisters may be added in order to gain more buoyancy to allow the increase of payload or the decrease of draft.

The superstructure deck or box–typed structure provides sufficient working space and deck area to load all the equipment and crew members required to carry out the intended functions of the floating structure. The deck or the box-typed structure also serve as a connection point that connects all columns together and also it transfers the loads to the columns located below. Depend on the designs, there may be a number of horizontal or diagonal braces connecting two columns or a column and the superstructure deck. The braces have different functions depend on the orientation but the main function is to strengthen the floating structure and support the deck weight. Some typical arrangements are shown in **Figure 2**.

The capability of a semi-submersible to stably support the maximum payload above the highest waves and with minimum responses to waves is the main factor that directly affect its sizing and dimension. The heave responses of the floating structure which is the most important degree of freedom depends on the ratio of pontoon to column volume and the structure must be designed in such a way that its natural period is not located within the range of most critical wave period of its operating locations to avoid resonance frequency.

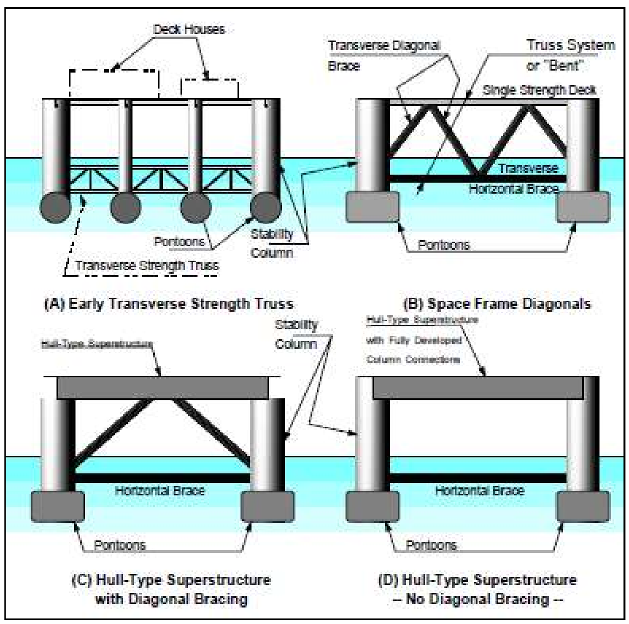

Figure 2 Semi-submersible Arrangement **[4]**

A semi-submersible is with minimum 20 years design life and usually more. During these years, the structure is exposed to environmental loadings, payload, and changes of water ballast due to different operating conditions. The cyclic loads bring possible fatigue problems and some of the critical locations which are considered sensitive to fatigue are the connections between column – pontoon and column – brace. Every welded joint and structural detail or other form of stress concentration is a potential source of fatigue cracking and should be taken into consideration as well. Fatigue assessment which is supported by a detailed fatigue analyses are performed to make sure that the structure exposed to extensive dynamic loading has an adequate fatigue life and the estimated fatigue life obtained through analyses is used as a basic for planning inspection and maintenance program during the operation life of the structure.

1.3 Objective and Scope of the thesis

The fatigue analysis of a semi-submersible is a huge and multidisciplinary engineering topic. In this thesis, the objective is more on the preliminary fatigue analysis on a semi-submersible hull. And thus, the scope of the thesis is narrowed down to below.

- Prepare FE models based on reference drawing given to identify the global responses of the structure and identify the critical areas based on results of hydrodynamic analysis.
- Perform a quick fatigue screening based on reference available in classification rules.
- Perform a stochastic fatigue analysis on the critical area which is extracted from the global model in form of global and sub-model to find out the fatigue usage factor and fatigue design life.
- Compare the possible differences in term of global responses and fatigue life for semi-submersible with and without sponsons attached to the columns.

The following thesis structure is organized, as shown below.

- For **chapter 2**, some basic theories related with fatigue analysis are discussed.
- For **chapter 3 & 4**, a brief introduction to the software package used in the thesis and the flowchart of methodology involving steps to be taken in each stage of analysis.
- For **chapter 5**, a summary on modelling works involved and also explanation on how the FE models are prepared, their loading and boundary conditions.
- For **chapter 6**, theories related with global response analysis and the necessary set-up required are briefly discussed. Also, the results from global response analysis are shown and discussed.
- For **chapter 7**, a quick fatigue screen is performed based on reference available in classification rules and the results are shown and discussed.
- For **chapter 8**, sub-model principle and the set-up of stochastic fatigue analysis is briefly discussed, together with the results of analysis.
- For **chapter 9**, the impacts of sponsons on overall fatigue and global response analysis are performed and discussed.
- For **chapter 10 & 11**, conclusion, further work and recommendation of the thesis.

2 FATIGUE THEORY

2.1 Introduction

During the service period of a semi-submersible, it experiences the extensive dynamic stress variations that are possible to initiate fatigue cracks if the welded joints or structural details are not properly designed or constructed. Without proper maintenance and solution, crack propagation may subsequently bring damage to primary structural members.

One of the practicable ways to assess the fatigue life of a structure is by using S-N curve. S-N curves are constructed mostly based on data collected from experiments conducted on different structural details in laboratories. The design S-N curves are based on the mean-minus-two-standard-deviation curves for relevant experimental data and thus the S-N curves are associated with a 97.7% probability of survival. The fatigue strength of welded joints is, to some extent, dependent on plate thickness and this effect is due to the local geometry of the weld toe in relation to thickness of the adjoining plates. The effect of thickness is taken into consideration by applying a modification on the stress range so that for any thickness larger than the reference thickness the design S-N curve is represented by equation below and K is the thickness exponent. [5]

$$\log N = \log \bar{a} - m \log\left(\Delta\sigma\left(\frac{t}{t_{ref}}\right)^{k}\right) \tag{2-1}$$

In S-N curves, the number of cycles (N) and the stress range (S) required to cause fatigue failure on a structural detail are presented. The fatigue life of a structural detail is estimated based on S-N curves under the assumption of linear cumulative damage (Palmgren-Miner rule). The accumulated fatigue damage is estimated using equation below.

$$D = \sum_{i=1}^{k} \frac{n_i}{N_i} = \frac{1}{\bar{a}} \sum_{i=1}^{k} n_i \cdot (\Delta\sigma_i)^m \tag{2-2}$$

Where n_i is the number of cycles the structural detail endures at stress range S_i and N_i is the number of cycles to failure at the stress range S_i, as determined by the appropriate S-N curve. k is the number of considered stress range interval.

There are a few types of S-N curves for fatigue analysis depending on the structural details and environmental conditions. Depending on the kind of stresses considered, the fatigue assessment is categorized into three approaches, 'nominal stress approach', 'hot spot stress approach' and 'notch stress approach'. Different S-N curves are used for different stress approaches.

2.2 Nominal Stress Approach

Nominal stress is the stress calculated in the sectional area under consideration, disregarding the local stress raising effects of the welded joint, but including the stress raising effects of the macro-geometric shape of the component in the vicinity of the joint. **Figure 3** below shows the examples of macrogeometric effects with stress concentrations at (a) cut-outs, (b) curved beams, (c) wide plate, (d) curved flanges, (e) concentrated loads and (f) excentricities.

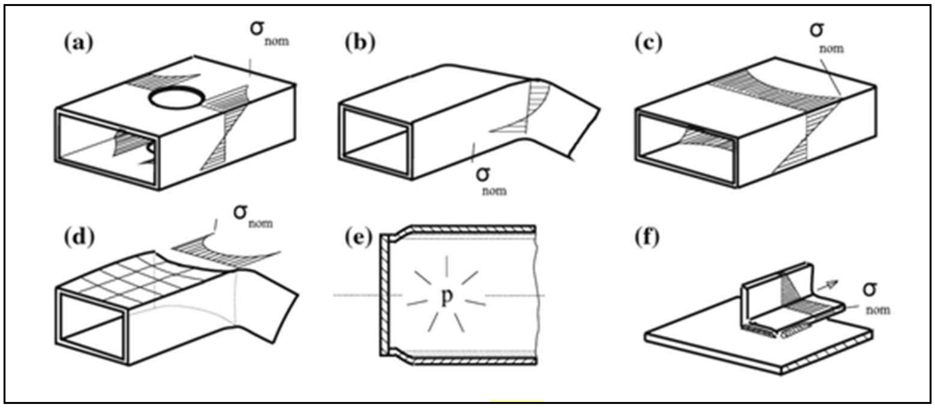

Figure 3 Examples of macrogeometric effects **[6]**

The nominal stress approach basically compare the nominal stress range amplitude of a structural detail with the nominal stress amplitude shown in S-N curve. For simple structural detail, the nominal stress is estimated with basic structural mechanic theories based on linear-elastic behavior. The stress range amplitude is defined as the equation below.

$$\Delta\sigma_n = \sigma_{max} - \sigma_{min} \qquad (2\text{-}3)$$

For structures in real life, particularly for welded structures, it is more common to have variable amplitude loading than constant amplitude loading, as shown in **Figure 4**. [7]

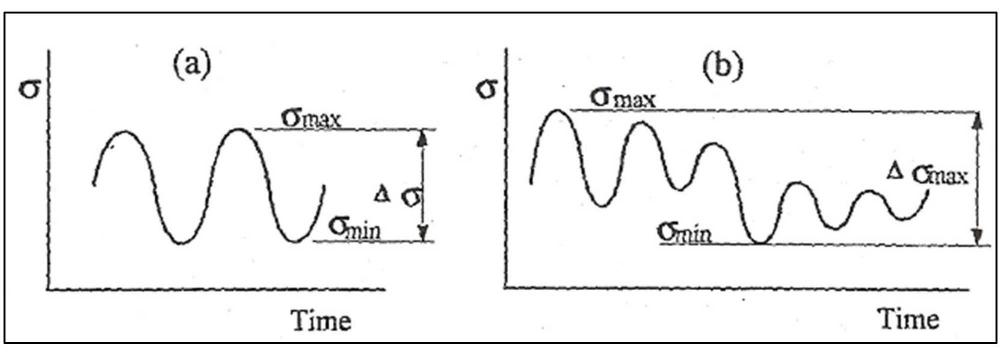

Figure 4 Constant (a) and variable (b) amplitude stress histories [7]

In summary, the fatigue life of a structural detail is calculated based on steps below.

1) Weld class is selected based on a given structural detail
2) Nominal stress range is calculated.
3) Stress range is corrected for thickness and misalignment effect.
4) Based on S-N curve, number of cycles to failure is determined.
5) Fatigue damage and anticipated fatigue life is calculated using Miner rule.

2.3 Hot Spot Stress Approach

The hot spot stress is a local stress at the weld toe, taking into account the overall geometry of the joint, except the shape of the weld. It is also called the structural or geometrical stress. Therefore, hotspot stress approach basically is to determine the structural stress at the toe of the weld, excluding the nonlinear component of the stress, which is referred in some codes as the stress peak. Depend on rules, two or three types of hotspot stress are usually defined, see **Figure 5.**

(a) At the weld toe on the plate surface at an ending attachment;

(b) At the weld toe around the plate edge of an ending attachment;

(c) Along the weld of an attached plate (weld toes on both the plate and attachment surface).

Based on DNV Notes 30-7 [8], the notch effect due to the weld is included in the S-N curve and the hot spot stress is derived by extrapolation of the structural stress to the reference points with a distance of 0.5 and 1.5 times the plate thickness. **Figure 6** below shows the schematic stress distribution at a hot spot.

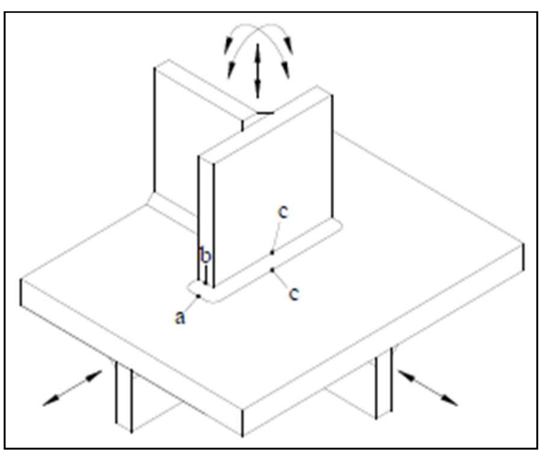

Figure 5 Different hot spot positions **[8]**

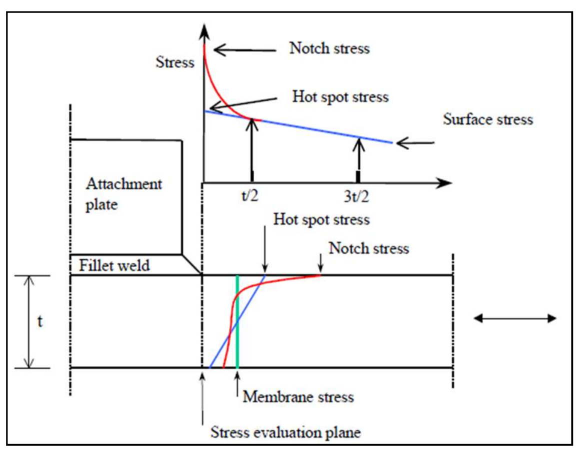

Figure 6 Schematic stress distribution at hot spot **[8]**

Hot spot stress obtained from finite element analysis (FEA) should take into consideration the possible misalignment and an appropriate stress concentration factor. Depending on the shape and size of the structure, shell or solid elements are used as mesh in FEA. As hotspot are usually located in an area with higher strain gradients and thus the FEA result is mesh sensitive. The size and type of elements used and how the values are extracted from elements are some of the possible reasons that affect the results significantly. Therefore, a proper method of extracting stress results from the FEA model must be selected. There are some detailed information about the meshing and determination of the hot spot stress mentioned in IIW and DNV fatigue design rules. Based on IIW, the recommended meshing and extrapolation methods are showed in **Figure 7** below.

Recommended meshing and extrapolation

Type of model and weld toe		Relatively coase models		Relatively fine models	
		Type a	Type b	Type a	Type b
Element size	Shells	t x t max t x w/2*)	10 x 10 mm	≤0.4 t x t or ≤0.4 t x w/2	≤ 4 x 4 mm
	Solids	t x t max t x w	10 x 10 mm	≤0.4 t x t or ≤0.4 t x w/2	≤ 4 x 4 mm
Extra-polation points	Shells	0.5 t and 1.5 t mid-side points**)	5 and 15 mm mid-side points	0.4 t and 1.0 t nodal points	4, 8 and 12 mm nodal points
	Solids	0.5 and 1.5 t surface center	5 and 15 mm surface center	0.4 t and 1.0 t nodal points	4, 8 and 12 mm nodal points

*) w = longitudinal attachment thickness + 2 weld leg lengths
**) surface center at transverse welds, if the weld below the plate is not modelled (see left part of fig. 2.2-11)

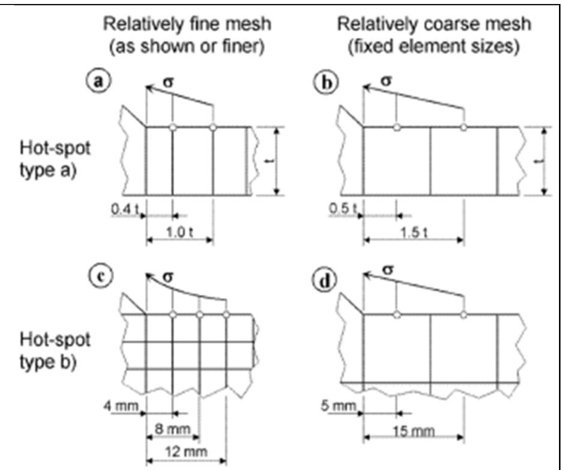

Figure 7 Recommended meshing and extrapolation **[6]**

2.4 Effective Notch Stress Approach

Based on DNV RP C203 [5], notch stress is the total stress at the root of a notch taking into account the stress concentration caused by the local notch and it consists of the sum of structural stress and non-linear stress peak. Effective notch stress approach is mainly based on the calculated highest elastic stress at the critical points which are also the crack initiation points. The real weld is replaced by an effective weld in order to take into consideration the statistical nature of weld shape parameters and non-linear material behavior at the notch root.

Under this approach, the stress range in a fictitious rounding in the weld toe or root is correlated to the corresponding fatigue life using S-N curves. FE model with reference radius of 1mm is typically used to obtain the notch stress and to avoid the stress singularities in sharp notches. [9] **Figure 8** below shows the illustration of the approach.

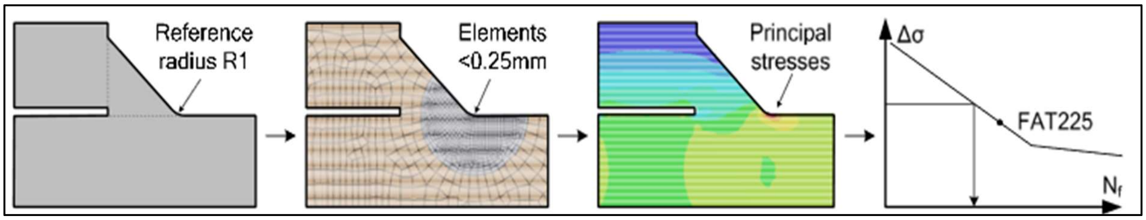

Figure 8 Schematic principles of fatigue assessment using the notch stress approach **[9]**

Similar to hot spot stress approach, when effective notch stress method is used for fatigue analysis of welded structural details, the elements on the areas concerned must be sufficiently dense so that the stress values at the concentration points are captured with sufficient accuracy. Particularly, the areas where possible crack initiation are expected to occur. Generally, 3-dimension elements are used unless the loading and geometry are simple then 2-dimension elements are used. The method is restricted to welded joints which are expected to fail from the weld toe or weld root and it is valid only for plate with thicknesses $t \geq 5$ mm.

2.5 Stress Concentration Factor

Under nominal stress approach, finite element model used for estimating nominal stress is of simple and coarse meshes (roughly about 3 times the thickness) [10]. For hotspot stress approach, as it is mesh-sensitive and in order to capture results with sufficient accuracy, smaller and finer elements (about 0.5 to 1.5 times the thickness) should be used for analysis purpose as mentioned in Section 2.2. The requirement of finer mesh leads to extra efforts needed in FE model preparation and all these must be done at the early stage of project when the model is being built.

Relations between different types of stresses may be established using stress concentration factors (SCF) as shown in equations below.

$$\sigma_{hs} = K_g \cdot \sigma_n \tag{2-4}$$

$$\sigma_p = K_g \cdot K_w \cdot \sigma_n \tag{2-5}$$

K_g is SCF due to the geometrical configuration of the connection and whereas K_w is SCF which includes effect associated to the weld geometry. K_g can be found by the FEA in which the nominal stresses in the structural parts is calculated, but it is for mesh dimension too coarse to represent local stress gradients. Some estimated values based on experimental results for typical details can also be found in rules. K_g is omitted if the FEA is sufficiently accurate to simulate the stress gradient caused by the structural details. K_w can be found by parametric formulas based on the results of finite element analyses and experiments.

2.6 The Simplified Fatigue Assessment Method

A simplified fatigue assessment method or deterministic approach is often used as fatigue screening technique in offshore engineering. Based on the screening results, if the structure's strength is adequate, no further analysis is required. More refined techniques are required for further analysis if the structural detail fails the screening criterion.

In the simplified fatigue assessment method, the linear long-term distribution of stress range may be modelled by using the two-parameter Weibull distribution. Where k and h are the Weibull scale and shape parameters respectively.

$$F(S) = 1 - e^{-(S/k)^h} \tag{2-6}$$

S_R is defined as the largest stress range anticipated in a reference number of stress cycles, N_R. The probability for S_R is shown in equation. The scale parameter, k is obtained by using equation below. The value of h is determined through a spectral fatigue analysis or measurements

$$P(S > S_R) = \frac{1}{N_R} \tag{2-7}$$

$$k = \frac{S_R}{(\ln N_R)^{1/h}} \tag{2-8}$$

In the simplified fatigue assessment method, the four main steps are shown below. The linear cumulative damage (Palmgren-Miner) rule is applied and the fatigue strength is defined by the S-N curves.

1. Determine the fatigue loads
2. Calculate the long-term distribution of stress range
3. Find the fatigue capacity of structure
4. Assess the fatigue damage

2.7 The Spectral-based Fatigue Assessment Method

The main concern with the deterministic method of calculating fatigue is that not all waves have the same period and wave length. Also, the stochastic nature of the environment is not really taken into account by assuming all waves are regular. Therefore, the results may be different from the actual site conditions. In contrast to simplified fatigue assessment method, spectral-based fatigue assessment method or stochastic fatigue analyses take into consideration the relevant site specific data and the directional probability of the environmental data. Possible wave spectra to apply in a stochastic (frequency domain) fatigue analysis are Jonswap, Pierson-Moskowitz, Gamma or Ochi-Hubble.

The spectral-based fatigue assessment method is a numerical intensive and complex method that able to produce results in terms of fatigue induced damage or fatigue life. Therefore, it is also referred to as a direct method. Some of the main assumptions used in this methods are as shown below. [11]

a) Since it is a frequency domain analysis, load and structural analysis are assumed to be linear. The scaling and superposition of stress range transfer functions from unit amplitude waves are considered valid.
b) Ocean wave is the main source of fatigue inducing stress range acting on the structure.
c) Structural dynamic amplification, transient loads and effect such as springing are considered insignificant.
d) Correction factors are used to treat the possible non-linearities due to non-linear roll motions and intermittent application of loads for example loads acting on side shell in the splash zone.

2.8 Time Domain Analysis

Based on the assumptions used, there are also some limitations in frequency domain analysis, for example, low-frequency fatigue stresses are difficult to predict and cannot take into consideration the nonlinearities of loads. Also, the results provide just the qualitative indication of the fatigue life of a structure and are not so accurate as compared to the Time-Domain analysis in which the irregular water surfaces would be simulated. However, time domain analysis has higher requirement of computational power and longer calculation time but for some offshore structures such as Tension Leg Platforms, time domain analysis together with the rain flow counting technique are used widely in the fatigue analysis. [11]

For time-domain analysis, the long term wave conditions considered are discretized into a number of representative sea-states of short duration and with constant intensity. Wave spectrum is used to generate the time history of the wave kinematics for the short duration. And then, based on the wave kinematics, hydrodynamic loads are calculated and then applied to the structural model. When structural analysis is performed, it is possible to estimate stress responses by taking into consideration the nonlinear effects. The number of stress cycles based on the stress time-history is estimated using the rain flow counting technique. [11]

2.9 Fatigue Life Improvement

Fatigue issue is more critical in ships built of high strength steel because the fatigue strength of steel in the as-weld condition does not increase in proportion to the yield and tensile strength [12]. The theory is applicable to offshore structures built with high strength steel as well. During the design stage, the improvement on the structure fatigue strength is generally performed through better design and arrangement. Structural designs with proper load transfer mechanisms through better proportioning and alignment of members help to improve stress continuity and reduce stress concentration. In fabrication process, there are some techniques that can be applied to improve the fatigue life of weld connection vulnerable to long term cyclic loading. Usually, these techniques reduce weld stress concentration factor or remove the defects at the weld toe. Others remove the harmful tensile welding residual stresses or introduce compressive stresses to increase the fatigue life [15]. Some of the widely adopted techniques in fatigue life improvement of welded connection offshore structure are grinding, weld toe re-melting, hammer and shot peening.

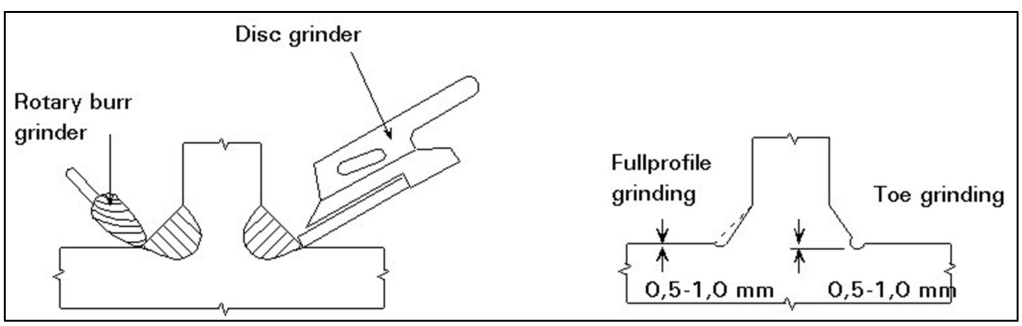

Figure 9 Different grinding methods and minimum depth required **[15]**

Grinding is performed using a rotary burr grinder or disc grinder and to ensure the removal of slag intrusions, usually grinding must be extended to a minimum of 0.5mm. See **Figure 9**. By lowering the stress concentration factor and removing weld toe defects, grinding is able to increase fatigue life for about 25 to 100%. Weld toe re-melting is usually conducted by using Tungsten Inert Gas (TIG) and plasma dressing. With the re-melting, slag inclusions and undercuts are removed, smoother weld toes transitions with smooth lower concentration factor could be obtained. The improvement of fatigue life is ranging from 10 to 100% depends primarily on the base material strength, joint severity and type of welding. [15] Hammer Peening and shot peening are some of the most widely used methods but the basic is the same. Peening is performed by deforming a metal surface by impacts and with these, compressive stresses are introduced to the material to improve the fatigue strength.

Table 1 below shows the increase in fatigue life by different methods given by DNV-GL. Based on [5], as there are always uncertainties regarding workmanship and quality assurance of the weld fatigue life improving process, the methods aforementioned are not recommendable for general use at the design stage.

Table 1 Fatigue life improvement of different methods **[5]**

Improvement method	Minimum specified yield strength	Increase in fatigue life (factor on life)
Grinding	Less than 350 MPa	0.1*fy
	Higher than 350 MPa	3.5
TIG dressing	Less than 350 MPa	0.1*fy
	Higher than 350 MPa	3.5
Hammer peening	Less than 350 MPa	0.011*fy
	Higher than 350 MPa	4.0

fy = characteristic yield strength for the actual material.

3 SOFTWARE

Undeniably, there is various software available in the market that can be used to perform structural and hydrodynamic analyses of ships and offshore floating structures. For modelling and analysis purpose, Sesam, a software suite developed by DNV-GL for the purpose of structural and hydrodynamic analyses for both ships and offshore structures is used here. The software suite consists of a number of modules and only some of them are used. A brief introduction of the modules that are used are shown below. For more details, the user manual of each modules are listed in reference.

GeniE is used for finite element modelling of beam, plate and shell of global or sub structures. The mass or FEM models needed for hydrodynamic and structural analyses are prepared using this software with different superelement. Sestra is the module in Sesam which is used to perform linear static and dynamic structural analysis by building up and solving the equations. Submod is a module that is used to transfer displacement from global model to sub-model and thus reduce complexity and time needed in preparing detailed sub-model.

HydroD is used for hydrodynamic and hydrostatic analysis of fixed and floating structures like offshore platforms and ships. Here in this thesis, only one of the HydroD module - Wadam is used for wave-structure interaction analysis in order to compute wave loads and motion response. Calculation of global responses like rigid body motions, first and second order wave exciting forces and moments, hydrodynamic added mass and damping can be performed using this module. Some of the results computed, like structural loads, are then transferred to the respective finite element model and the global response results generated including offbody points, panel pressures and cross sectional loads are then recorded an hydrodynamic results interface file which is typically used by Postresp, Stofat and Xtract for further processing and analysis.

Figure 10 shows the modules under Sesam and based on the functions of the modules, it can be categorized into 5 groups. Depend on the complication of an analysis, a number of module from different groups maybe combined and used to perform calculation.

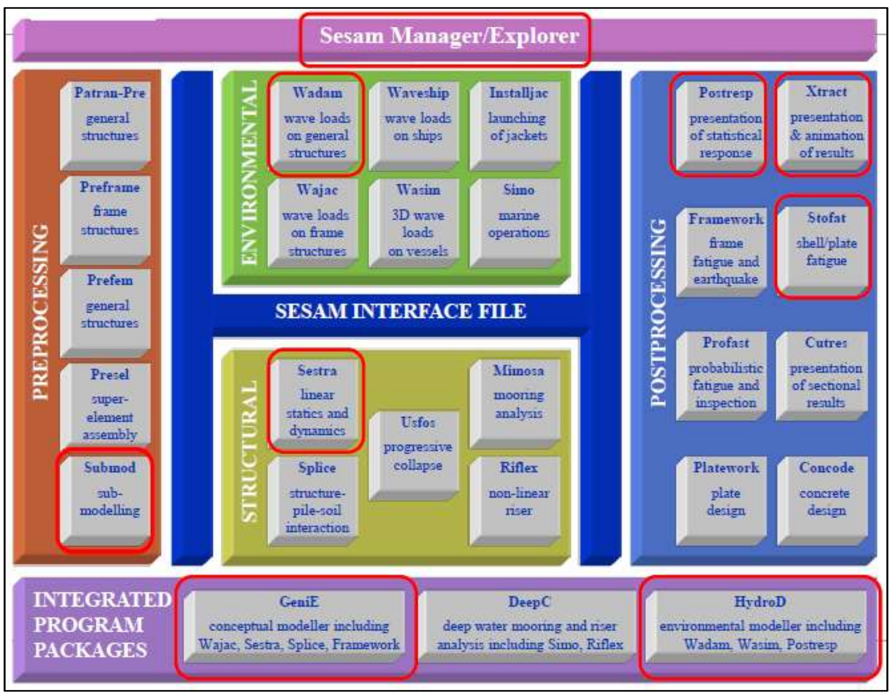

Figure 10 Modules of Sesam **[16]**

Xtract is a module which is used to visualize and further process FE structural and hydrodynamic models and results whereas Postresp is a module which is used as a postprocessor for statistical responses calculations. These two modules are used to prepare graphs, figures, and animations for result verification and report writing.

Stofat is a module which is used to perform stochastic fatigue calculation of both welded shell and plate structures modelled by 3D shell and solid elements by postprocessing the hydrodynamic results interface file generated by HydroD and Sestra. The stresses generated by hydrodynamic loads due to a number of different wave directions and frequencies are recorded as stress transfer functions in the results interface file. Fatigue damages calculation at given points in the structural model are performed based on the results. And then, SN-curve based fatigue approach is used and partial damages over different sea states and wave directions are accumulated. With these, the usage factor during a certain period and fatigue life of a structure are calculated.

4 METHODOLOGY

Based on ABS rules, for semi-submersibles which are considered as column-stabilized floating installations, the wave and current induced load components are not dominated by the drag component. Therefore, there is a linear relationship between wave height and stress range and a special set of method is provided. Spectral-based fatigue analysis is performed to check the fatigue life and the key components of the method for the selected structural locations can be categorized into the following components:

a. Establish fatigue demand
b. Determine fatigue strength or capacity
c. Calculate fatigue damage or expected life

In order to establish fatigue demand, the stress transfer function or stress RAOs for locations in the structure is established. Information like environmental data and load conditions are then incorporated to produce stress response spectra, which are used to derive the magnitude and frequency of occurrence of local stress ranges at the locations for which fatigue damage is to be calculated. The results are then compared with the fatigue strength or capacity which are estimated by using S-N curves to calculate the expected life. **Figure 11** shows the detailed procedures for ABS spectral-based fatigue analysis procedure.

Based on DNV-GL rules, a full stochastic fatigue analysis of a global model is performed to calculate the fatigue life of a structure. Linear load effects and responses are assumed in the spectral method. The hydrodynamic loads and structural responses are calculated using 3D potential theory and finite element analysis respectively. The detailed procedures for full stochastic analysis of global model are shown in **Figure 12** and the procedures involved can generally [12] be divided into 4 large groups, modelling, analysis, post-processing and reporting.

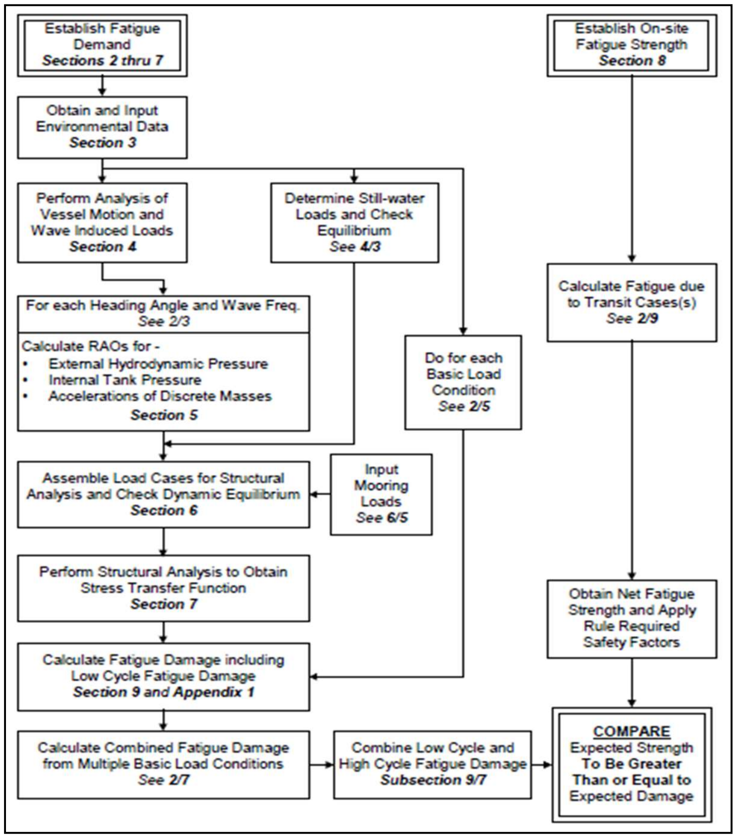

Figure 11 Schematic Spectral-based Fatigue Analysis Procedure **[13]**

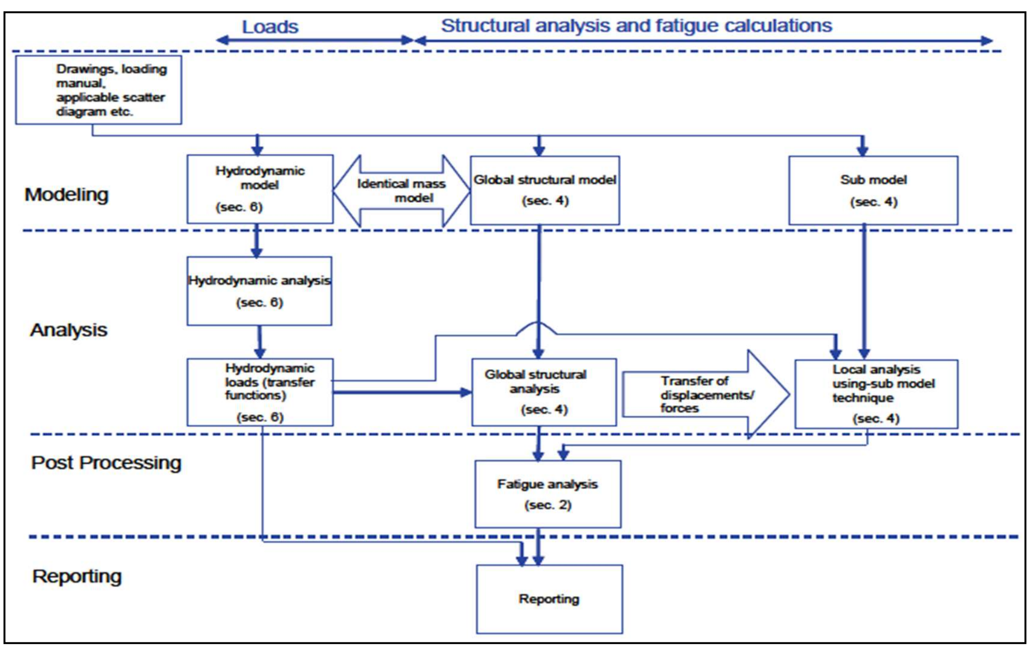

Figure 12 Full Stochastic Analysis Procedure Flowchart – Global Model **[14]**

For this thesis, the DNV-GL rules are used as a guidance and by taking into consideration the different modules of Sesam to be used during each stage of analysis, the flowchart showing the steps involved in the fatigue analysis is shown **Figure 13**.

For the very first step, GeniE is used to prepare the finite element models required for further hydrodynamic and structural analyses. There is a total of 4 models needed, namely mass model, structural model, panel model and Morison model. Consideration that must be taken into account while preparing the model are further discussed in Section 5.

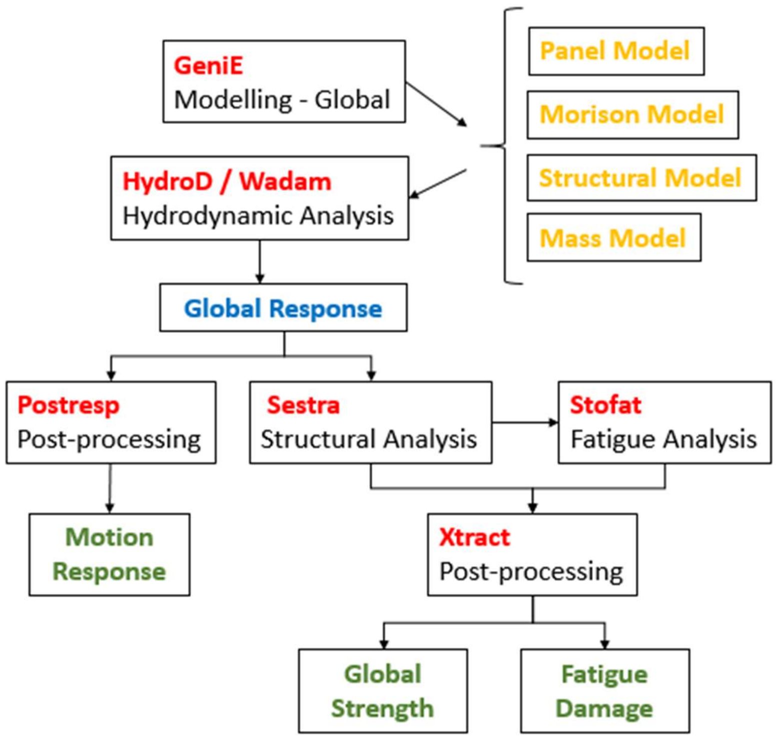

Figure 13 Flowchart of analyses with modules of Sesam to be used

After that, by combining all available models, hydrodynamic analysis is performed using hydroD, particularly Wadam. The environmental conditions for the model to be tested is determined taking into consideration various factors. Global responses are obtained as results of the hydrodynamics analysis. Motion responses including 3 translational motions (heave, sway and surge) and 3 rotational motions (pitch, roll and yaw) of the unit are obtained by post-processing the global responses using the Postresp.

Sestra is used to perform structural analysis taking into account the global responses generated by the hydrodynamic analysis. Output from the structural analysis to be used as input in Stofat to perform stochastic fatigue analysis. After that, output from Sestra and Stofat are post-processed in Xtract to visualize the global strength and also the cumulated fatigue damage or usage factor of the unit.

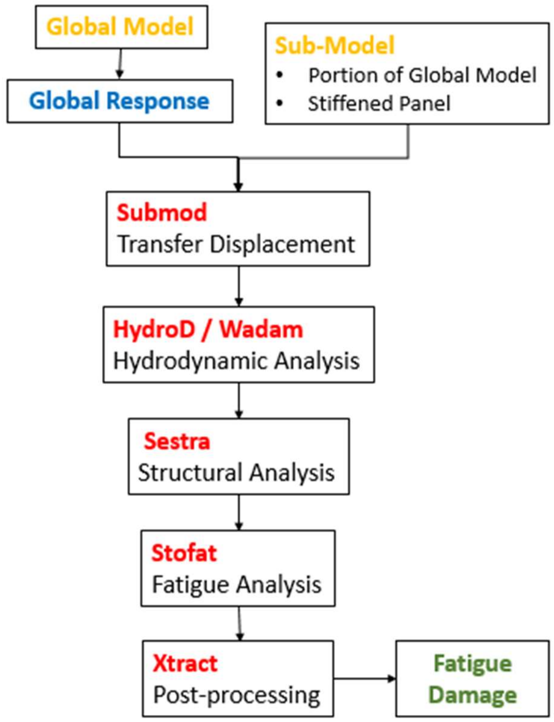

Figure 14 Flowchart of analyses involved sub-model

The fatigue analyses on sub-model in forms of stiffened panel or portion of global model are performed based on the flowchart shown in the **Figure 14** above. By using the global response result file, displacement is transferred to the sub-model using Submod. After that, the sub-model is used as a structural model in HydroD for hydrodynamic analysis. Finally, structural and fatigue analyses are performed in the same way as per the global model.

In the last part, the same hydrodynamic and fatigue analyses are performed on the same semi-submersible without sponsons to check the possible impact of sponsons, FE models are modified and adjusted accordingly. Similar to previous procedures, the results obtained are post-processed and visualized using respective modules.

5 MODEL PREPARATION

5.1 Model Dimension

The semi-submersible to be analysed here is a ring pontoon semi-submersible with four similar pontoons arranged in a ring-shape. The main dimensions are as shown in **Table 2** below.

Table 2 Specification

Pontoon Length	85m
Pontoon Breath	85m
Pontoon Height	12m
Column Length	17.5m
Column Breath	17.5m
Depth to Deck Box Bottom	40.5m
Draught, operating	27.5m

5.2 Panel Model

Panel model is used for the calculation of the 3D wave potential in Wadam. Only the wet surfaces are being modelled here and interior surfaces which are not exposed to sea water are not considered here. Differences in element sizes used for modelling cause the differences in computation time. Obviously, more time is required if there are more elements. In addition, it is important to take into consideration whether the shape and hull details can be modelled out properly using limited number of elements. Sufficient elements are needed in order to ensure that the important shape and hull details are properly modelled and the generation of reliable computation results.

In preparing the panel model, a quick check is performed on different element sizes ranging from 2m to 6m to check whether there is any possible difference on the motion generated by Wadam. Element with size 1m is omitted from motion analysis as the maximum number of panel for Wadam is exceeded. A summary of element size and its respective number of element in a panel model is shown in table below. The heave RAO generated by different panel models of different element sizes are compared and shown in Table **3**.

Table 3 Element Size vs Number of Element

Element Size (m)	Number of Element
1	24526
2	7038
3	4201
4	2426
5	1705
6	1377

Based on the **Figure 15**, noticed that the heave amplitude for different element sizes are almost the same except for wave period from 18s to 27s. The range of resonance period based on different element sizes are from 22s to 24s. The mesh size directly determine how detailed the wetted surface is considered in analysis. Bigger elements may not be sufficiently detailed in representing the curve shape especially if the shape is smaller than the size of element.

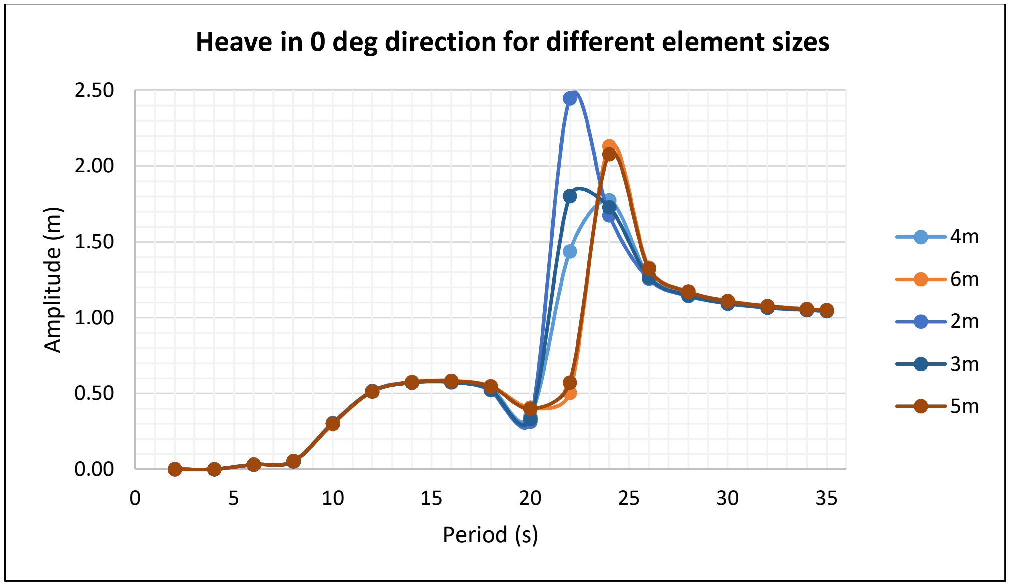

Figure 15 Heave in 0 degree direction for different element sizes

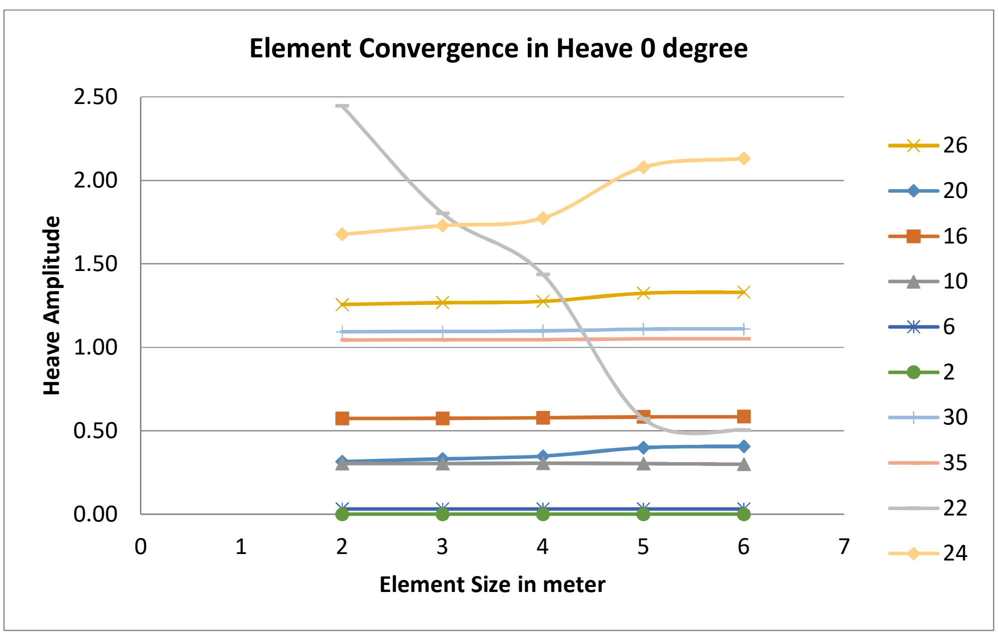

Figure 16 Element Convergence in Heave 0 degree

A check on the convergence of the results is shown in **Figure 16** and noticed that the results given by different sizes of elements are actually quite close for most of the wave periods except between 22s to 24s. Element size of 4m is selected for further analysis.

Based on [17], the uncouple natural period in heave for a freely floating vessel can be estimated using Equation **(5-1)**. The added mass coefficient is estimated based on tables attached in the appendix of [18] and with the coefficient, the added mass can be calculated using Equation **(5-2)**.

$$T_3 = 2\pi\left(\frac{M + A_{33}}{\rho g S}\right)^{\frac{1}{2}} \tag{5-1}$$

$$A_{33} = C_A * \rho * \pi * b^2 * l \tag{5-2}$$

The width to height ratio of pontoon is calculated (=8.75/6 = 1.458). C_A (=1.44) is then estimated by interpolating between width to height ratio of 1 and 2.With C_A and the total length of pontoons , the total added mass of pontoons is calculated as shown in Equation **(5-3)**. After that, the heave resonance period is calculated in Equation **(5-4)**. Noticed that the results from Wadam is close to the results based on rule calculation.

$$A_{33} = 1.44 * 1025 * \pi * 8.75^2 * 320 = 1.14x10^8 kg \tag{5-3}$$

$$T_3 = 2 * \pi\left(\frac{8x10^7 + 1.14\,x10^8}{1025 * 9.81 * 1382}\right)^{\frac{1}{2}} = 23.5s \tag{5-4}$$

5.3 Morison Model

The Morison model is used to calculate wave forces, added mass and drag damping calculation using Morison theory. Morison model is modelled in such a way that it closely resemble the panel model as Wadam calculates the hydrostatic load based on this model alone in a load transfer analysis. Both Morison and Panel model are with same span so that all wetted panels of the panel model are connected to beams in the Morison model. The Morison model is prepared using beam element to represent both pontoons and columns with elements modelled as 2 node beams. The input of added mass coefficient and drag coefficient used in the modelling of Morison Model are as shown in **Table 4**.

Table 4 added mass coefficient and drag coefficient used

	C_{DY}	C_{DZ}	C_{AY}	C_{AZ}
Column	2.2	2.2	0.497	0.497
Pontoon	2.2	2.2	1.435	1.435

Figure 17 shows the Morison model of the semi-submersible in 2 node beam element. **Figure 18** shows the correspondence between panel and Morison model when dual model method is used in which all the panels are connected to Morison elements.

5.4 Structural Model

5.4.1 Modelling

The structural model is prepared based on the hull drawings with some reasonable simplification. As the focus here is more on the wetted surface below water line. The internal bulkheads and structural details inside column and pontoon are simplified. In the real case, there are some differences in structural details among the four columns, as well as the four pontoons. But, in this report, all pontoons and columns are assumed to be the same. In addition, the deck box which is exposed to air and located on top of columns are modelled with only plates and without beams as it is used only to transfer the loads of point masses to columns. Some other assumptions made in preparing structural model are listed below.

a) Minor opening and penetration on main bulkhead like manholes and hatches are not modeled assuming that the reinforcement added around the penetration is able to keep the strength of the structure.
b) Steel structures which are parts of steel outfitting are not considered.
c) Brackets and stiffeners at certain curvy areas are not modelled in the global structural model but only considered in detailed sub-model analysis.
d) Patches of insert plates added on side shells of pontoons and columns for local reinforcement, for example the insert plate below bollards, are not considered.

For an actual ring pontoon unit, steel plates with different material grades are used in different locations of the unit depending on the structural category of the locations. The grade of steel to be used is related to the service temperature and thickness for the applicable structural category as mentioned in [19]. For simplification, all material for the unit is assumed with material properties shown in **Table 5** . Thickness of plates used in modelling is shown in **Figure 22** after some simplification based on the assumptions aforementioned.

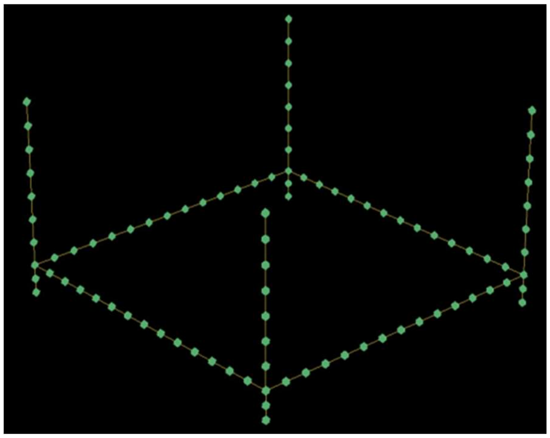

Figure 17 Morison Model

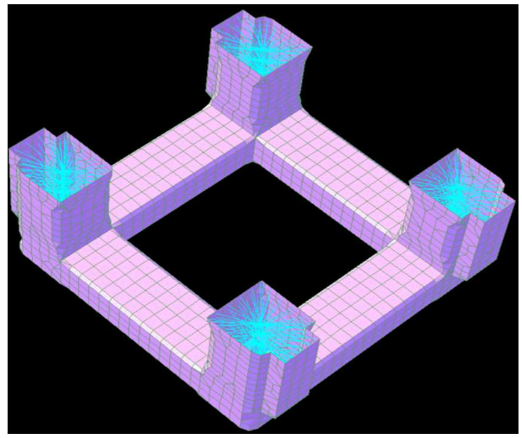

Figure 18 Correspondence between panel and Morison model

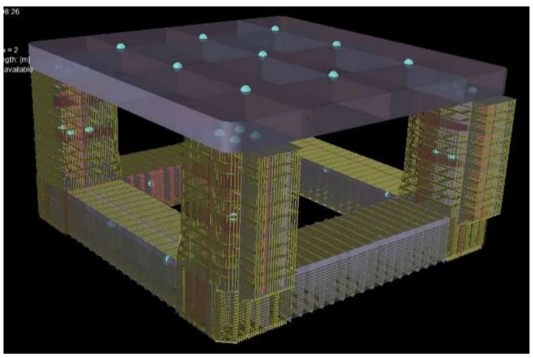

Figure 19 Structure model with point masses

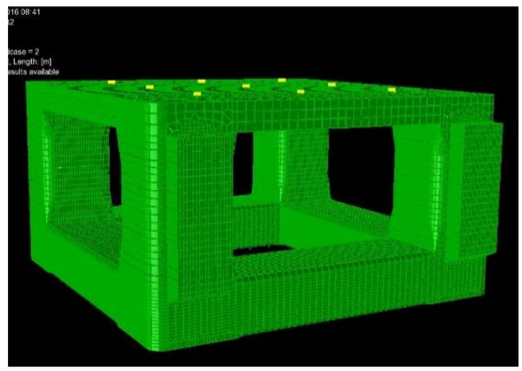

Figure 20 Structural model in finite element

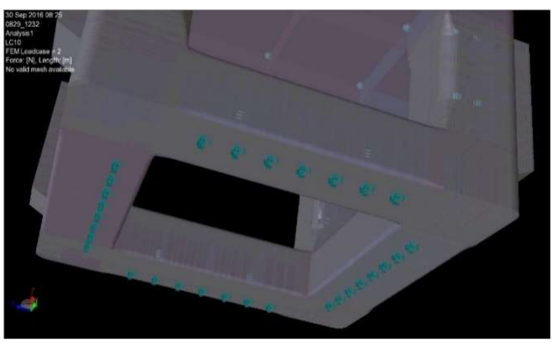

Figure 21 Model boundary conditions

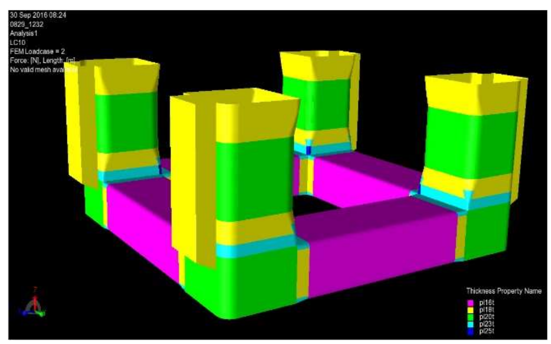

Figure 22 Plate thickness

Table 5 Material properties

Yield Stress	350MPa
Density	7850 kg/m^3
Young Modulus	2.1x10E11 Pa
Poisson Ratio	0.3

5.4.2 Meshing

Girders and stiffeners are modelled in beam element whereas side shells and bulkhead are modelled in shell element. Element type used in the modelling is second order element with 8 nodes. There are also some triangular elements in the model as the use of triangular elements is unavoidable at some complicated structural details but the number is kept to minimum.

The default maximum angle and relative Jacobi values in default meshing rules are applied to ensure that the elements are always in good shape that can generate reliable results. Model idealization is then performed to eliminate small edges which are misaligned to give better element shape. There are three types of built-in face mesher in GeniE, Sesam Quad Mesher (SQM) which is targeting slender and regular structure is selected. Under SQM, surfaces are divided into smaller patches and on top of the patches, meshes are created. Best mesh generated by SQM are generally found in the middle of a patch.

The size of mesh used in structural model is 2m x 2m but almost all wetted surface are with elements sizes which are smaller or equaled to the size of stiffener spacing which is 0.625m especially locations with more complicated details, for example, the connection point between pontoons and columns. The deck box located on top of columns is modelled in only plates as its main purpose is for equal load transfer to four supporting columns and the focus is on the structure below.

5.5 Mass model & Loading Condition

Based on **[20]**, a number of different loading conditions simulating static load distribution for each draft should be taken into consideration in the global model. In this case, we are more interested on the structural response in operating condition. Therefore, only one loading condition is considered here and thus the mass model is included in the structural model.

The operating draft of reference vessel is 27.5 m from baseline and the total displacement is about 81,000Mt at operating draft. The displacement is further broken down to lightship weight about 48,234Mt and 32,766Mt of payload and ballast. In preparing the structure model, there is no further breakdown to lightship weight, payload or ballast as not all steel structures are modelled. The weight of all steel structures modelled is taken into consideration and point masses are added to simulate the required loading condition in order to achieve the required draft. The point masses are distributed on deck box, columns and pontoons. Loads generated by ballast water, fuel oil and other liquid load in tanks of pontoon and column are simulated with point masses as well. Also, point masses are used to simulate the mooring loads in the analysis.

Appropriate locations are selected to locate the point masses to ensure that the loads are transferred from the deck box, through columns to the pontoons below. In addition, the center gravity of the model in X, Y and Z directions are carefully adjusted to match the actual model. The summary of both weight and centers of gravity for the reference and the model is shown in Table 6. The point masses in model are shown in **Figure 19**.

Table 6 Reference vs Model

Reference			Model		
Operating Draft	27.50	m	Operating Draft	27.28	m
Displacement	81000	MT	Displacement	80073	MT
Lightship	48234	MT	Structural Weight	13973	MT
Payload+ Ballast	32766	MT	Point Mass	66100	MT
VCG (Fr Baseline)	29.14	m	VCG (Fr Baseline)	29.24	m
TCG (Fwd+)	0.03	m	TCG (Fwd+)	-0.01	m
LCG (Port+)	-0.04	m	LCG (Port+)	0.01	m

5.6 Boundary Conditions

Based on [20], At least six degrees of freedom have to be fixed in order to avoid rigid body motion of a global structural model. There are two ways to apply the boundary conditions depending on whether the boundary conditions are statically determined or statically undetermined.

For the statically determined boundary conditions, six restraints are needed. By applying these conditions, unbalance in loads due to hydrodynamic pressure and model acceleration must be solved to avoid unphysical support reactions. For the statically undetermined boundary conditions, spring stiffness is calculated based on water plane area and unbalance in loads are distributed over several points. Springs to be located at strong points to limit the effect of reaction forces. The statically determined and undetermined boundary conditions of a twin-pontoon semi-submersible are shown in **Figure 23** and **Figure 24**. [20]

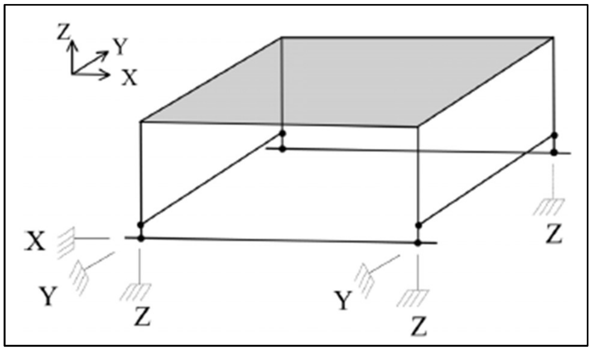

Figure 23 Statically determined boundary conditions **[20]**

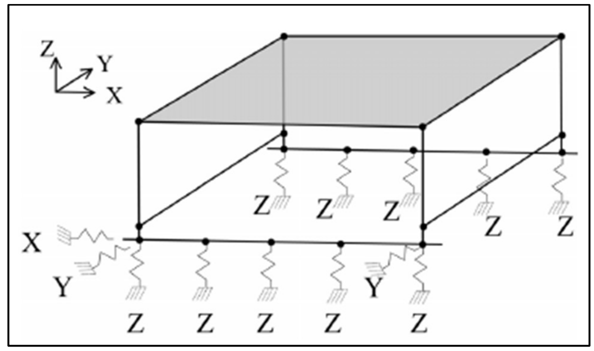

Figure 24 Statically undetermined boundary conditions **[20]**

For this analysis, statically undetermined boundary conditions are used. The spring stiffness required for the model is calculated using the Equation **(5-5)** below.

$$k = \rho g A_w \tag{5-5}$$

The water plane area based on the operating draft of model is 1382m^2 and thus the spring stiffness is about 1.39E^{7}N/m. The support points are located below the intersection between pontoon longitudinal and transverse bulkhead/girders. There is a total of 28 support points and they are distributed equally on four pontoons, as shown in figure below. All support points are with spring stiffness in Z direction and without rotational spring stiffness. As shown in **Figure 21**, there are two special points with the first point with spring stiffness in both Y and Z whereas the second point is with spring stiffness in all X, Y and Z directions. Horizontal spring stiffness is assumed as 1% of the vertical stiffness.

6 GLOBAL RESPONSE ANALYSIS

6.1 Introduction

The equation of motion for a floating structure can be written as Equation **(6-1)**.

$$[M]\ddot{X} = F_{WS} + F_{gravity} + F_{moorings} + F_{others} \tag{6-1}$$

$\boldsymbol{F_{WS}}$ are forces due to wave and structure interaction.

$\boldsymbol{F_{gravity}}$ are gravity forces.

$\boldsymbol{F_{moorings}}$ are mooring forces.

$\boldsymbol{F_{others}}$ are other forces such as viscous forces.

$\boldsymbol{F_{WS}}$ can be further expanded to excitation forces ($\boldsymbol{F_{ex}}$), drag forces ($\boldsymbol{F_{drag}}$), radiation forces ($\boldsymbol{F_{radiation}}$) and hydrostatic forces ($\boldsymbol{-K_H X}$). The expanded equation is shown below.

$$[M]\ddot{X} = (-K_H X + F_{ex} + F_{radiation} + F_{drag}) \quad + F_{gravity} + F_{moorings} + F_{others} \tag{6-2}$$

Whether or not all the expanded terms of forces due to wave and structure interaction are taken into account depend on Keulegan Carpenter Number calculated using following equation.

$$KC = \frac{2\pi A}{L} \tag{6-3}$$

If the KC number is large (>10), there is a flow separation and incident flow is not perturbed much. And thus drag forces are dominating and diffraction/radiation forces are negligible. On contrary, when the KC number is small (< 2), the flow is attached to the body and there is a large perturbation of the incident flow. Under these conditions, diffraction/radiation forces are most important and the effect of drag forces is important only at resonance. For KC number between 2 and 10, the behavior is between the two cases depend on how big the number is.

For a twin pontoon semi-submersible, the pontoon is usually with low KC number and the braces that joining two pontoons together are with high KC number. Therefore, for pontoons, the diffraction/radiation effects are more dominating and, for braces, drag force are more dominating. Potential theory is used to calculate the diffraction/radiation effects and Morison equation for the drag forces. Whereas for ring-pontoon semi-submersible without braces, dominating diffraction/radiation effects on pontoons are analyzed.

Response analyses can be performed in two ways either frequency or time domain. Frequency-domain analysis refers to calculation of loads and responses in the frequency domain by solving the equations of motion using methods of harmonic analysis or methods of Laplace and Fourier transformations whereas Time-domain analysis refers to calculation of the loads and responses in the time domain. [21]

Based on rules, a frequency domain procedure is the most suitable for response analysis of column stabilized units **[20]** and thus instead of time domain analysis, this procedure is selected for this thesis.

Frequency-domain analysis which is a linear analysis system is used here. The equations of motions are solved for each of the incoming regular wave components for a wave frequency analysis, The output from a traditional radiation/diffraction frequency domain analysis are given as response amplitude per unit wave amplitude for excitation forces/moments, added mass/moments and potential damping and motion RAOs. **[22]**

In HydroD/Wadam, there are a few methods to study the global response analysis - panel model, composite model and dual model, as shown in **Figure 25**. Dual model is used here to include the pontoon viscous drag from Morison's equation to the damping terms calculated from potential theory as it is one of the most important damping contribution. Under this method, the legs and pontoons are modelled by both a beam (Morison) model and a panel model. The dual model is then defined by giving a relation between the panels and the beam elements. When such a model is used, Wadam computes the buoyancy and added mass from the panel model and only includes the drag term from the Morison model.

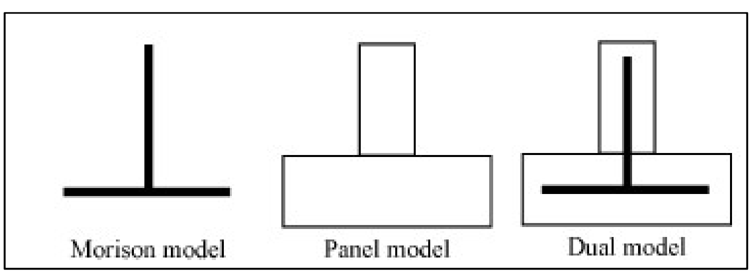

Figure 25 Hydro model combination

There are a total of three types of load calculated in the global response analysis.

1. Gravity load which is the weight of structure and also the load distributed on the structure.

2. Hydrostatic loads due to external loads in form of sea water acting on the side shells in the still water condition.

3. Hydrodynamic loads due to with contributions from exciting forces from incident waves, forces from wave induced motion and rigid body accelerations

6.2 Analysis Set-up

The sea water density is set at 1025 kg/m^3 with kinematic viscosity $\mathbf{1.19 \times 10^{-6} m^2/s}$. There is insufficient information about the exact location of the unit and thus the water depth is set at 300m.

For current load, it depends on local topographic conditions with often strong variability in magnitude and direction with depth and thus its calculation is challenging and access to local measurement data is needed. For wind loads acting on the structure, usually wind tunnel tests are conducted to estimate the wind loading in a sufficient number of wind directions and then the selection of wind spectrum that can represent the geographical area where the unit is located. **[22]** For the analysis here, the effect of wind and current loads on the structure are assumed to be negligible for the overall hull strength. Only static and wave induced loads are considered for stress distribution calculation.

Based on [20], a Pierson-Moskowitz (PM) wave spectrum representing fully developed seas is applicable in case the growth of the waves is not limited by the size of the generation area. The PM wave spectrum give acceptable results provided that the spectrum peak period is not close to a resonance peak in the response transfer function. [20] On the other hand, based on ABS rules, energy distribution among wave components of different frequencies of a sea state can be described by using either Bretschneider or JONSWAP. Frequency characteristics of the wave must be taken into account when selecting the suitable wave spectrum. Bretschneider spectrum is for open ocean areas with fully-developed seas and is usually used to describe tropical storm waves, such as those generated by hurricanes in the Gulf of Mexico. The JONSWAP spectrum is for fetch-limited regions and it is usually used to describe winter storm waves of the North Sea. [13]

For this analysis, Bretschneider wave spectrum or 2 parameter PM wave spectrum, with the Equation **(6-4)** as show below is used. **Figure 26** shows the graph of Bretschneider wave spectrum.

$$S(\omega) = \frac{5}{16}\frac{\omega_m^4}{\omega^5} H_{1/3}^2 e^{-5\omega_m^4/4\omega^4} \tag{6-4}$$

To simulate a short term wave condition, sea state duration is set as 3 hours. This duration is acceptable as based on rules, it is common to assume that the sea surface is stationary for a duration of 20 minutes to 3 or 6 hours. A stationary sea state can then be characterized by using environmental parameters such as the significant wave height Hs and the peak period Tp. [18] For the hydrodynamic analyses, significant wave height (13.6m) and peak period (16s) of 100 years return period for central North Sea sites based on ISO 19901-1 is used.

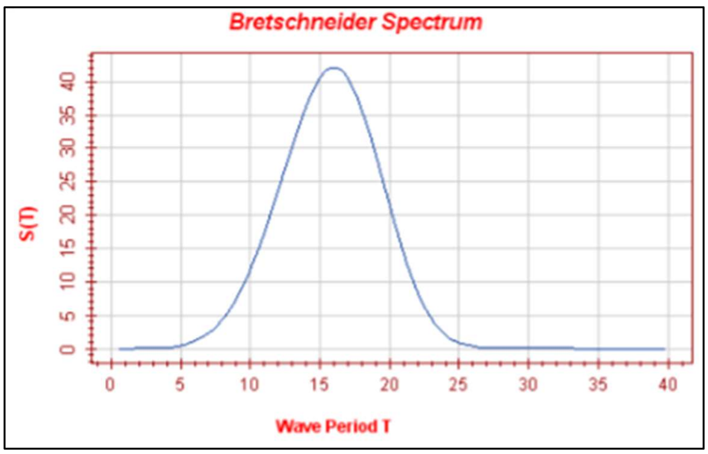

Figure 26 Bretschneider spectrum

The wave energy spreading function is introduced to account for the energy spreading among directions for a short crested sea. Real sea waves are not infinitely long crested and directional spectra are required for a complete statistical description of the sea. One of the common methods to obtain the two-dimensional energy spectrum is through its expression as the product of the one-dimensional energy spectrum and its angular distribution function at each frequency [23]

$$S_\eta(f,\theta) = S_\eta(f) \times D(f,\theta) \tag{6-5}$$

$D(f,\theta)$ from the equation above is spreading function and it is usually simplified.

$$D(f,\theta) = D(\theta) \tag{6-6}$$

Some of the example of spreading functions are as shown in Equation **(6-7*)*** and **(6-8**) below. **[24]**

$$D(\theta) = \frac{2^{2s-1}}{\pi}\frac{\Gamma^2(s+1)}{\Gamma(2s+1)}cos^{2s}\left(\frac{\theta-\theta_m}{2}\right), -\pi \leq \theta-\theta_m \leq \pi \qquad (6\text{-}7)$$

$$D(\theta) = \frac{1}{\sqrt{2\pi\sigma}}exp\left(\frac{(\theta-\theta_m)^2}{2\sigma^2}\right), -\pi \leq \theta-\theta_m \leq \pi \qquad (6\text{-}8)$$

s is spreading parameter,

Γ is gamma function,

θ_m is mean direction and

σ is spreading angle.

Based on rules, the effect of wave short-crestedness may be included in a stochastic wave load analysis by introducing a wave energy spreading function in the calculation. For the fatigue analysis of a column-stabilized unit, PM wave spectrum with a $\boldsymbol{cos^4\alpha}$ wave spreading function should be used, with $\boldsymbol{\alpha}$ which is the angle between direction of elementary wave trains and the main direction of the short-crested wave system. **[20]**Therefore, the wave energy spreading function is chosen as $\cos^4(\theta)$ as requested and the wave spreading direction is set as 0 degree. The wave spreading functions for different values of cosine power N is shown in **Figure 27**. **[25]**

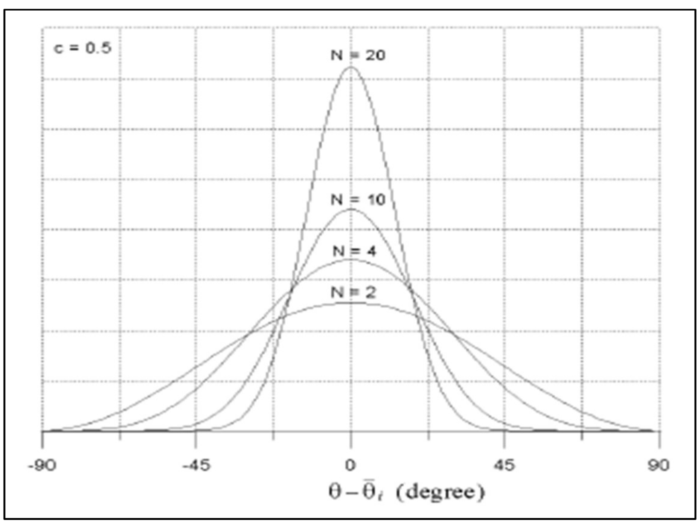

Figure 27 Wave spreading functions for different values of cosine N **[25]**

Drag term for pontoon is linearized by stochastic method even it is less dominated in comparison to the hydrodynamic inertia forces due to wave loading **[20]**. Based on **[22]**, selection of wave periods for the wave frequency analysis is usually done with basis in:

- Peak period in wave spectrum
- Location of rigid body Eigen periods
- Geometrical considerations (diameters of columns, spacing between columns, length/width)

The main objective is to describe the actual RAOs with a sufficient number of wave periods and wave headings. Regular Wave period ranging from 2s to 28s with 3s gap are considered in the analyses. Based on Section 5.2 above, the heave period is somewhere around 22-24, with estimation using manual calculation showing results of about 23.5s. The wave period of 23 second is therefore included in the frequency range. The corresponding wave length and direction of the selected wave set are summarized in table below. The direction considered in the analysis is ranging from 0° to 315° with gap of 45°. With these, there is a total of 80 load cases consists of a direction set of 8 and a frequency set of 10. The wave periods selected and their corresponding frequency and wave length are shown in **Table 7**.

Table 7 Selection of wave periods

	Wave Period	Frequency	Wave Length
	(s)	(Hz)	(m)
1	2	0.50	6.24
2	5	0.20	39.02
3	8	0.13	99.89
4	11	0.09	188.85
5	14	0.07	305.91
6	17	0.06	451.06
7	20	0.05	624.31
8	23	0.04	825.65
9	26	0.04	1055.09
10	28	0.04	1223.65

Selection of wave periods based on geometric consideration is taken into account together with the characteristic global response of the floating unit. Therefore, wave load on structure is studied in two set of load cases.

a) Set of regular wave and frequency with same gap

b) Characteristic global response

6.2.1 Characteristic Global Response

Based on **[20]**, there are some global responses that are governing for global strength of a ring pontoon units, as shown in **Figure 28**. The analysis is somehow different form a twin pontoon semi-submersible. For ring pontoon unit, only the split force (F_S), torsion moment (M_t), vertical wave bending moment on the pontoons and shear force (F_L) related to both transverse and longitudinal axes are considered here.

For a ring pontoon unit, split force contribute to axial force and bending moments in the pontoon with maximum responses at the mid-section and pontoon end. The critical value occurs at beam sea of 90° and a wave length of about twice the outer breath between pontoon. Characteristic response due to deck mass acceleration are not considered here due to the insufficient data on actual weight distribution and incompleteness of deck box model.

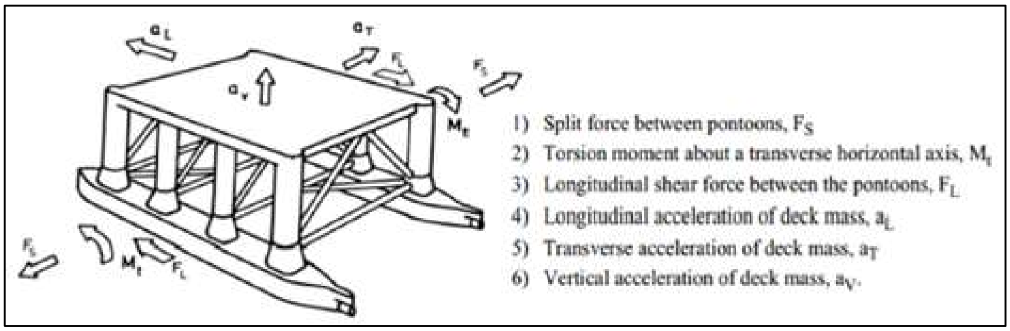

Figure 28 Characteristic global response **[20]**

The vertical wave bending moment on the pontoon achieves maximum value at head sea condition with critical wave length slightly larger than the pontoon length.

The torsion moment gives the maximum responses are at the pontoon/ node/ column intersections. The critical value for this response occurs at a diagonal wave with heading between 45° to 60° and the wave length is approximately the distance of the diagonal distance between the pontoon ends. Usually the responses due to torsion moment are lesser than longitudinal/transversal shear forces and split forces and forces for a ring pontoon unit. The longitudinal shear force between the pontoons normally occurs at a wave heading between 45 to 60 degree and with wave length about 1.5 times the distance of the diagonal distance between the ends of pontoon. **[20]**

There are a total of 28 load cases and load cases shown in **Table 8** are prepared based on the 4 types of characteristic global responses mentioned above. All load cases (LCs) are named with

3 digits in order to differentiate them from the previous set of load case. As four pontoons joined together to form a ring pontoon unit, beam sea and head sea condition for each pontoon are different. Therefore, split force and vertical wave bending are considered in 4 directions and respective wave length. The critical wave length of vertical wave bending moment are assumed to be 5% or 10% longer than the pontoon length. For torsion moment and longitudinal shear force, in addition to 45° and 60°, two more directions – 50° & 55° which are between 45° and 60° are considered as well. In addition, as a ring pontoon unit have extra two pontoons which are arranged perpendicular to the only two pontoons the unit would have, if it is a twin pontoon unit, so 4 extra directions are added.

Table 8 Load cases for characteristic global response

LC	Responses	Angle (deg)	Wave Length (m)
101	Split forces between pontoons	0	130
102		90	
103		180	
104		270	
105	Vertical wave bending moment on the pontoon	0	84
106		90	
107		180	
108		270	
109		0	88
110		90	
111		180	
112		270	

LC	Responses	Angle (deg)	Wave Length (m)
113	Torsion Moment	45	95.46
114		50	
115		55	
116		60	
117		135	
118		140	
119		145	
120		150	
121	Longitudinal Shear Force between the pontoons	45	143.19
122		50	
123		55	
124		60	
125		135	
126		140	
127		145	
128		150	

6.3 Results

6.3.1 Motion

Based on **[22]** part 2.2, semi-submersibles are usually with “softer” horizontal plane with the natural period of surge, sway and yaw generally longer than 100s whereas the heave is usually slightly over 20 seconds due to the small water plane area. The response amplitude operators (RAO) in six degrees of freedoms under head sea (0°) are shown below. Noticed that yaw, sway and roll are almost negligible. And heave is the major motion response that affect the unit with the maximum heave of about 1.6 and the period is about 23s.

6.3.2 Hydrodynamic Analysis

The stress distribution due to the combination of gravity load and hydrostatics load are shown in **Figure 30**. The maximum responses of the total 108 load cases (=80 +28) mentioned previously are combined and shown in **Figure 31**. The combined maximum hydrodynamic stress due to different load cases are obtained by scanning through each and every of the load cases and get the maximum values .These values are not the exact hydrodynamic load acting on the structure but the values give a conservative estimation on the maximum stresses on the unit.

Noticed that generally the hydrodynamic load is lesser in comparison to the combination of gravity load and hydrostatics load. A quick check here is performed by using the partial load factors of ultimate limit states mentioned in **[26]**, the partial load factors are shown below. For combination-a, the load factor for permanent & variable functional loads are taken as 1.3 as the load is not well defined in terms of distribution and with great uncertainty.

Table 9 Partial load factors of Ultimate Limit States **[26]**

Combination	Load Categories	
	Permanent & Variable functional loads	Environmental loads
a	1.3*	0.7
b	1	1.2

The stress distribution under combination-a and b are shown in following figures and noticed that combination-a is more stringent due to higher contribution from gravity load and hydrostatics load.

In addition, it is noticeable that higher stresses are concentrating on the connection point between pontoon/column. Internal column side shells, Pontoon inner and outer side shells adjacent to the connection point of pontoon/column also experience higher stress in comparison to pontoon top plates and sponsons. With material yield stress of 340 N/mm^2 and material safety factor of 1.15 **[26]**, the allowable von Mises stress is about 295M/mm^2. Generally, the resultant stresses are below the allowable von Mises. **Table 10** shows the summary of the von Mises stress on each part of the unit based on load combination-a.

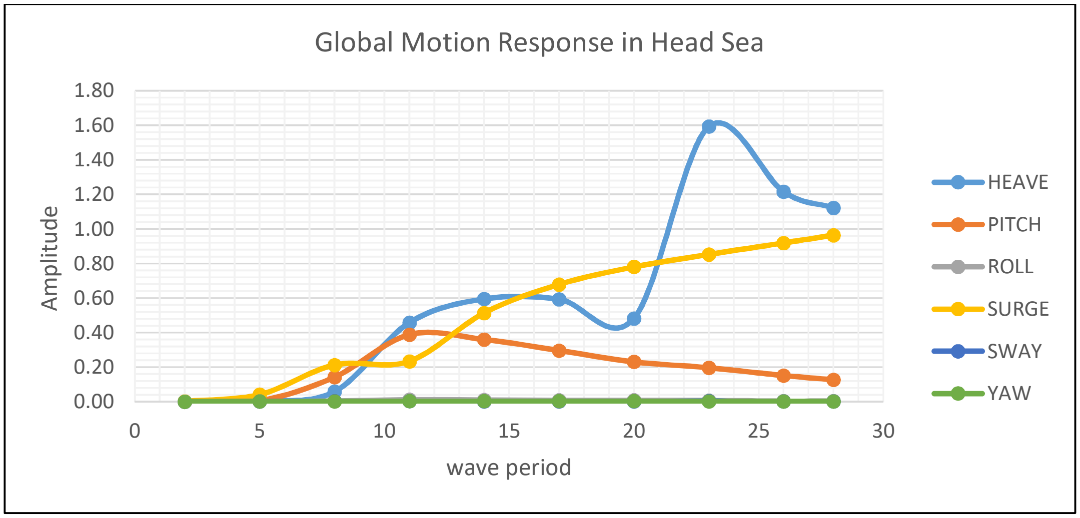

Figure 29 Global motion response in head sea

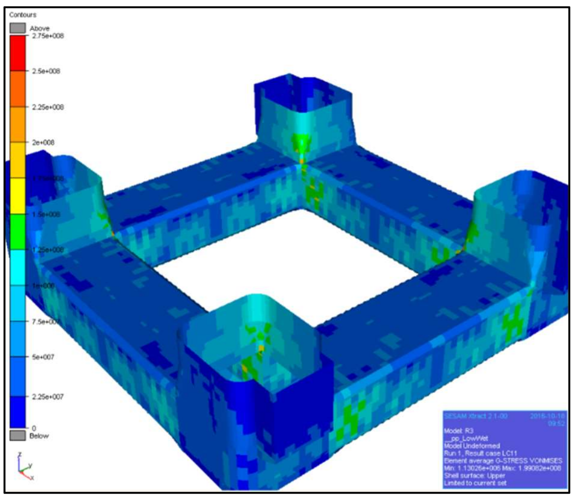

Figure 30 Combination of gravity and hydrostatics load

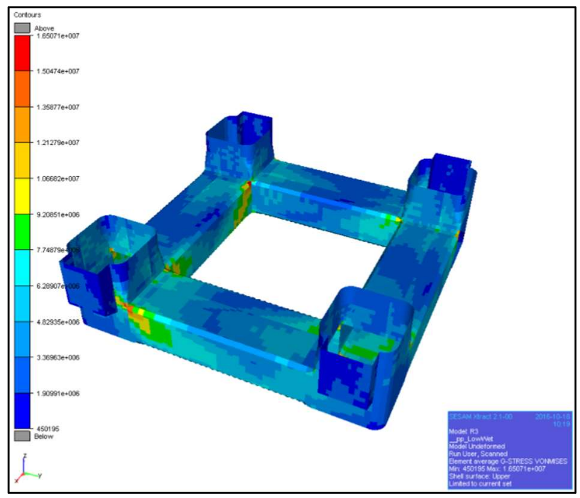

Figure 31 Combination of all load cases

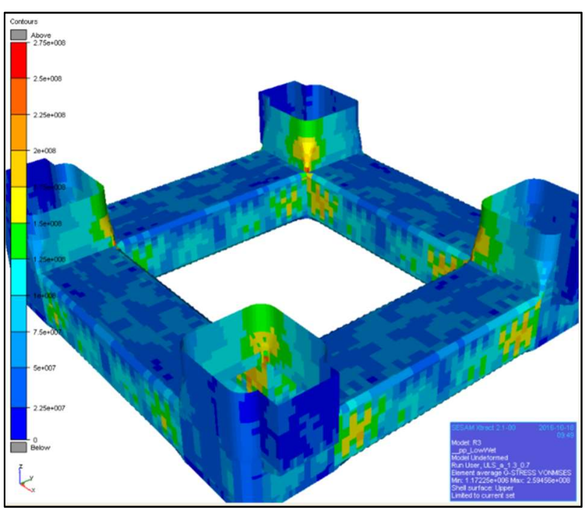

Figure 32 ULS Combination-a

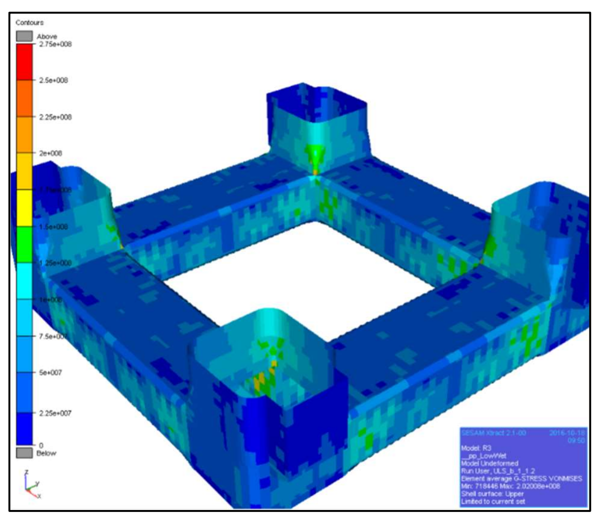

Figure 33 ULS Combination-b

Table 10 Summary of von Mises stress distribution

No	Location	Stress Range (N/mm^2)
1	Pontoon Top Plate	< 125
2	Pontoon Bottom Plate	<150
3	Pontoon vertical side shell near columns	< 200
4	Pontoon-Column connection point	<275
5	Column side shell facing inwards	< 225
6	Column side shell facing outwards	< 125
7	Sponson	< 100

7 QUICK SCREEN CHECK FOR FATIGUE

7.1 Introduction

In order to have a better idea of possible stress range for the structure, a quick screen check for fatigue is performed based on the examples and charts given in **[5]**. The calculation example in is used to estimate the allowable extreme stress range for the model during 10^8 cycles (20 years' service life which corresponds to an average cycling period of 6.3 sec) **[5]**. Design charts shown in **[5]** are used to determine the allowable stress range.

Due to the difficulty in predicting the actual fatigue life of offshore structure, a safety factor called design fatigue factor (DFF) is used to cover the possible uncertainty. The value of DFF depends on how significant the structural components are with respect to the overall structural integrity and availability for inspection and repair. The calculated fatigue life of a structure must be at any time longer than DFF times the design life. Based on **[19]**, the DFF for a structure that is with low consequence of failure and satisfies the class requirement on accident limit state is as shown in **Table 11** below. Noticed that the highest safety factor of 3 is used for non-accessible areas. There are other rules with more stringent requirement for example NORSOK (N-001), a safety factor of 10 is used for non-accessible are with substantial consequence of failure. The NORSOK rules is shown in **Table 12**.

The unit design life is 20 years and taken into consideration that majority of the structure considered in the analysis are external side shells that could be assessed by changing the draft of the semi-submersible to lower or transit draft, the DFF is assumed to be 2.

Table 11 Design Fatigue Factor based on **[19]**

DFF	Structural element
1	Internal structure, accessible and not welded directly to the submerged part.
1	External structure, accessible for regular inspection and repair in dry and clean conditions.
2	Internal structure, accessible and welded directly to the submerged part.
2	External structure not accessible for inspection and repair in dry and clean conditions.
3	Non-accessible areas, areas not planned to be accessible for inspection and repair during operation.

Table 12 Design Fatigue Factor based on NORSOK N-001 **[27]**

Classification of structural components based on damage consequence	Not accessible for inspection and repair or in the splash	Accessible for inspection, change or repair and where inspection or change is assumed	
		Below splash zone	Above splash zone or internal
Substantial Consequences	10	3	2
Without substantial consequences	3	2	1

There are different classes of S-N curves used in fatigue analysis. Each curve represents a class of weld details and the differences are depending on a few factors as listed below. [28]

- Geometrical arrangement of the structural detail
- Direction of the fluctuating stress relative to the detail,
- Method of fabrication and inspection of the detail

The selection of S-N curve is based on the structural details to be considered in fatigue analysis. For a semi-submersible, there are many structural details that need to be analyzed using different S-N curve. In order to simplify the analysis, the S-N curve class F is used for the fatigue screening. In addition, there are some factors such as residual stresses, the presence of notches, corrosion and temperature that affect the progression of the S-N curve [29]. As the part of structure concerned is the part that submerged below sea surface so, instead of S-N curve in air, S-N curves for sea water environment with cathodic protection are selected as the curves better represent the environmental conditions. The number of fatigue cycles with corresponding fatigue stress of the S-N curve class F selected is shown in **Figure 34** together with other classes of S-N curve.

The maximum thickness of the steel plates is assumed to be 25.0 mm. A Weibull shape parameter, h, of 1 is assumed. By using h =1, the allowable stress range of 191.1N/mm^2 is obtained. This result is based on allowable stress for 20 years design life and a Design Fatigue Factors (DFF) equal 1. For any DFF larger than one the allowable fatigue limit should be reduced by a factor (DFF)$^{-0.33}$.

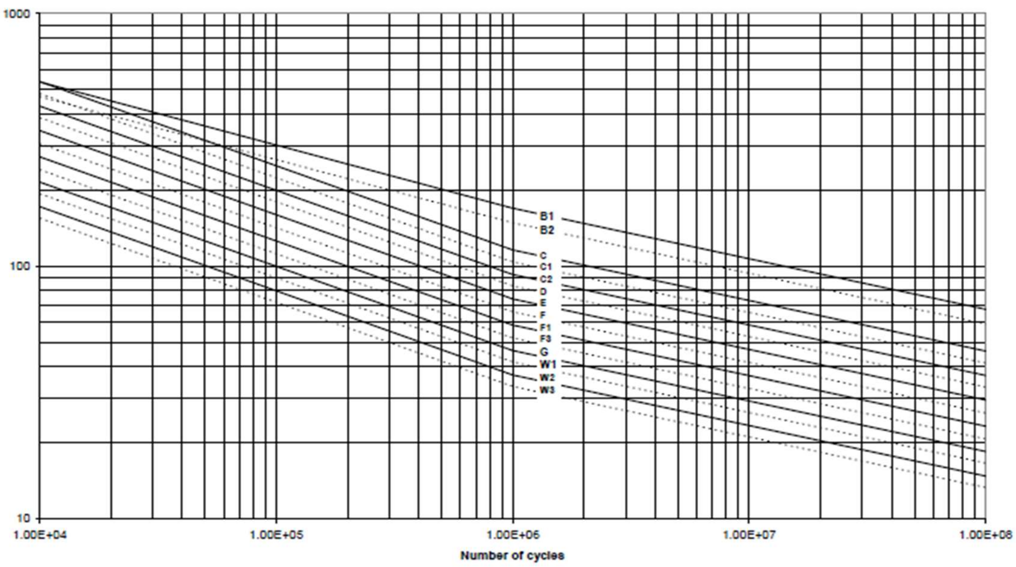

Figure 34 S-N curves in seawater with cathodic protection **[5]**

By taking into consideration a DFF equal 2, the utilization factor η which is equal to 0.5 is obtained. A reduction factor of 0.938 is then obtained based on the utilization factor η and the weilbull shape parameter. The allowable stress range for a 25 mm thick plate is obtained by taken into consideration the reduction factor as 191.1*0.858 = 163.96 N/mm^2. With the same approach, the allowable stress with different plate thickness are calculated taking into consideration the thickness exponent k as shown in **Table 13**. Noticed that due to thickness effect, the weld allowable stress decreases if the thickness of load-carrying plate increases.

Table 13 Allowable stress for different plate thickness

Plate thickness (mm)	16	18	20	23	25
Allowable Stress (N/mm^2)	183.32	178.00	173.37	167.42	163.96

7.2 Discussion

By comparing the results of quick screening, plate thickness and the stress distribution shown in combination a mentioned in Section 6.3.2, noticed that the area with stresses higher than the allowable stress range can be narrowed down into only a few areas. These areas are Pontoon vertical side shell near columns, Pontoon-Column connection point and Column side shell facing moon pool. These areas are selected for further investigation using stochastic fatigue analysis to get better results.

Based on rules [5], the shape parameter h in the Weibull distribution has a crucial impact on fatigue damage calculation. In this part, it is assumed as 1.0 but it is just as assumption. By using S-N curve class F for sea water environment with cathodic protection, the impact of Weibull shape parameter on the allowable stress range is shown in **Table 14** and **Table 15** below. Noticed that the shape parameter h in the Weibull distribution has some impact on allowable stress for different plate thickness. When the Weibull parameter is lower, allowable stress for a same plate thickness is lower as well. Therefore, for a more conservative study, a lower Weibull shape parameter can be used in estimating the allowable stress. In order to see the impact of different S-N curve on the allowable stress, S-N curve class C is selected and the whole calculation is repeated. The results are shown in **Table 15**, noticed that even the same Weibull shape parameter is used, the allowable stress can be very different if the S-N curve class is different.

Based on rules [5], depending on the types of S-N curve applied, if the largest local stress range of an area of interest is less than the fatigue limit at 10^7 cycles, a detailed fatigue analysis is omitted. It means that under such a stress level, the failure of material is impossible and theoretically the cycle can be repeated infinitely. As curve F is used here, the fatigue limit at 10^7 cycles for this curve is 41.52 MPa. Therefore, for area with local stress lesser than 41.52MPa, no detailed fatigue analysis is required.

Table 14 Allowable stress for S-N curve class F with different Weibull parameter

	Weibull Parameter	0.8	0.9	1	1.1	1.2
	Reduction Factor on stress	0.847	0.853	0.858	0.862	0.864
	Allowable stress range during 10^8 cycles for components in seawater with cathodic protection	263.60	221.40	191.10	168.60	151.30
	Allowable stress for 25mm thick plate, N/mm2	223.27	188.85	163.96	145.33	130.72
		Allowable stress, N/mm2				
Plate thickness in mm	25	223.27	188.85	163.96	145.33	130.72
	23	227.97	192.83	167.42	148.39	133.48
	20	236.08	199.69	173.37	153.67	138.22
	18	242.38	205.02	178.00	157.77	141.91
	16	249.62	211.15	183.32	162.49	146.15

Table 15 Allowable stress for S-N curve class C with different Weibull parameter

	Weibull Parameter	0.8	0.9	1	1.1	1.2
	Reduction Factor on stress	0.847	0.853	0.858	0.862	0.864
	Allowable stress range during 10^8 cycles for components in seawater with cathodic protection	464.30	389.80	336.70	297.00	266.50
	Allowable stress for 25mm thick plate, N/mm2	393.26	332.50	288.89	256.01	230.26
		Allowable stress, N/mm2				
Plate thickness in mm	25	393.26	332.50	288.89	256.01	230.26
	23	401.55	339.50	294.97	261.41	235.11
	20	415.82	351.58	305.46	270.70	243.47
	18	426.92	360.96	313.62	277.93	249.96
	16	439.68	371.75	322.99	286.23	257.43

8 STOCHASTIC FATIGUE ANALYSIS

8.1 Introduction

By performing a simplified fatigue analysis above, we roughly have an idea about which part of structure are more vulnerable to fatigue and where we should put more attention into. In addition, the maximum stress range of the structure is estimated.

Stochastic fatigue analyses are performed using DNV-GL software Stofat. As mentioned in the user manual **[25]**, for the structure to be analyzed using Stofat, the structure should be modelled sufficiently in terms of structural details and the distribution of force is correctly represented. The size of the model must be large enough that the stress distribution in critical areas is not affected by the loads and boundary conditions applied on the model. Here, the stochastic fatigue analysis is performed in two methods depend on the results required.

1) Using a global model with mesh size ranging from coarse (on the parts far from the region of interest) to fine (region of interest).
2) Using a sub-model with fine mesh to look into detail a small part of the whole structure. The sub-model may be in the form of stiffened plate or other structural parts.

Based on the methods used, there are possible impacts on the accuracy of the results and also total time needed for calculation. Using a global model with coarse mesh size is definitely faster as compared to a model with finer mesh size but in order to find the hotspot stress, there are some recommended element size to be used in meshing. For example, if hot spot stress approach to be used in fatigue analysis then the element size must be selected in according to the table shown in **Figure 7** above.

Generally speaking, the use of different element sizes in a FE model is possible given that the FE software is more powerful nowadays. However, the growth rate of element must be smooth to ensure a better FE model. It can be challenging for complicated structure details. Moreover, more effort and time are required for modelling in order to create better meshes.

8.2 Sub-model Principle

Sub-modelling is a technique used for refined and fast analysis of structural details. Usually, the technique involves transferring displacements from an analysis of an existing global model and impose the displacements as prescribed displacements on a sub-model which is a part belonging to the global model. In simple words, with this technique, the results from the global model are interpolated and extracted and then all of these are applied onto the sub-model. The size of finite element mesh is finer for sub-model and more accurate results can be produced within the sub-model region. The sub-model can be a combination of a few panels or a small block of interest. Depend on how detailed an analysis is, a global model can contain numerous sub-models.

For the analysis of semi-submersible with sponsons here, the sub-model is a portion of global model consists one of the four columns and half-length of pontoon in X and Y directions. Like mentioned above, prescribed displacements are applied on the boundaries of the column and pontoons to transfer displacement from global model, as shown in **Figure 36**.

Elements with size of 0.5m are applied for the whole sub-model while finer elements with size of 0.1m are applied on a volume of 5m x 5m x 5m with the center of volume located on the connection point between pontoon and column. The stiffeners and brackets located within the mentioned volume, which are omitted and simplified in global model, are modelled into shell elements while other stiffeners outside of the concerned volume are kept in beam elements. **Figure 35** shows the mentioned stiffeners and brackets.

8.3 Stofat Setup

In reality, the direction of sea waves within a short period of time is not always the same. In Stofat, a wave energy spreading function is assumed to be independent of the wave frequency and the wave energy is assumed to be spread over a set of directions +90 to -90 degrees on both sides of each main wave direction. If no wave spreading function is assigned, long crested waves are assumed as default setting. **[25]** Similar to hydrodynamic analysis performed above, the spreading function is assumed to be $\cos^4(\theta)$ as mentioned in **[20]**.

The directions of wave considered in Stofat are from zero to 315 degree with constant 45° gap between. The contribution of wave from each of the 8 directions to overall fatigue damage is assumed to be the same. Each direction contribute 12.5% of the fatigue damage to make the cumulative total damage 100%. This is just an assumption, if there are detailed site measurement data about the probability of wave direction for a specific location for a certain period of time, a better estimation of the direction probability can be done and a more accurate results may be obtained.

For long term analysis, wave scatter diagram is required. Stofat build-in wave scatter diagram of North Atlantic Sea is used. The wave scatter diagram is attached in the Section 15.1. There is a possibility that waves from different directions are with different wave height and period. It is possible here to consider those differences by using different sets of wave scatter diagram for different directions. However, for analyses in this report, waves from all directions are assumed to be complying with the North Atlantic Sea wave scatter diagram.

Similar to the quick screen performed in Section 7, S-N curve type F for sea water environment with cathodic protection is used and the stress concentration factor is assumed to 1.0.

There is a limitation on the number of elements in a single Stofat run and the problem size increases when there is an increase in the number of sea states, wave direction or elements. Table shown in Appendices Section 15.4 shows the maximum number of elements that may be included in a Stofat run. By using the existing computers in lab, the fatigue analyses are performed with about 5000 to 10000 elements each run.

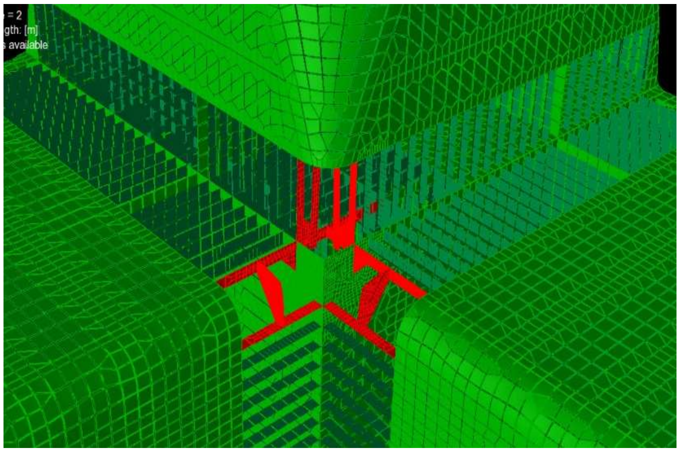

Figure 35 Stiffeners and brackets in shell element

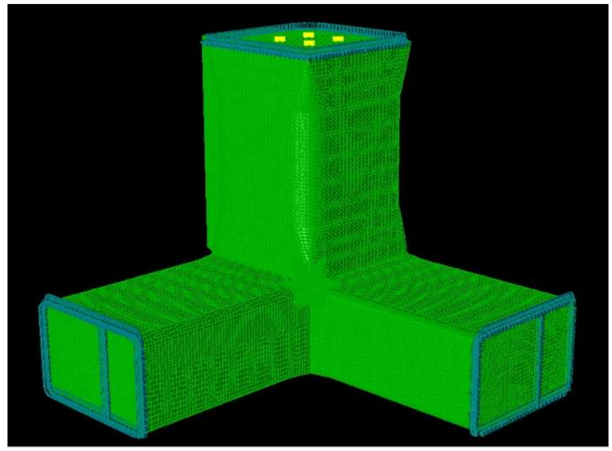

Figure 36 Sub-model FE model with boundary conditions

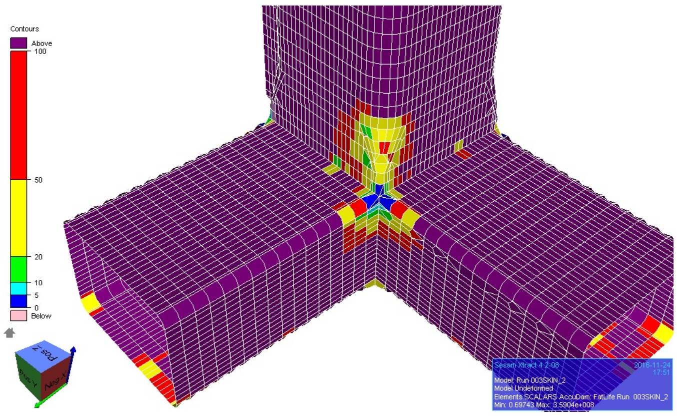

Figure 37 Fatigue life01 (Global Model – with sponsons)

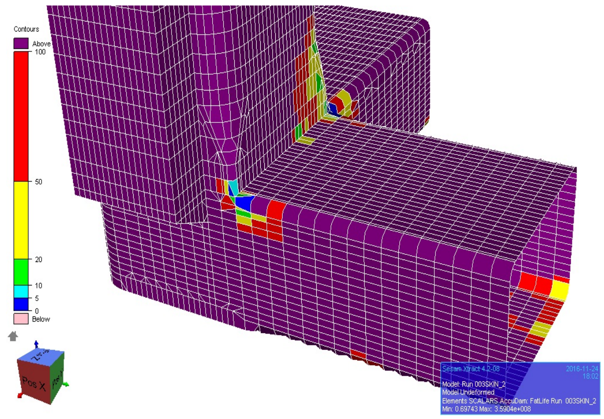

Figure 38 Fatigue life02 (Global Model- with sponsons)

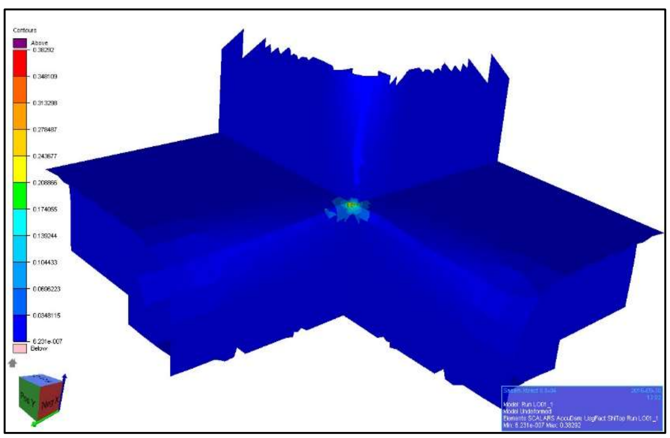

Figure 39 Fatigue usage factor (sub-model looking inboard)

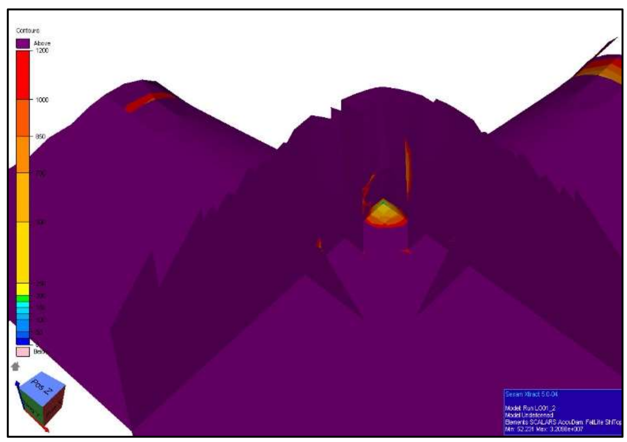

Figure 40 Fatigue life (sub-model looking outboard)

8.4 Results

Figure 37 and **Figure 38** show the stochastic fatigue analysis using global model. Noticed that some parts are with fatigue life lower than the minimum required design life of at least 20 years such as the pontoon-column connection facing inwards (**Figure 37**) and those on the side shells that facing outboard (**Figure 38**) which are the critical areas. For the rest, the fatigue life is generally 20 years and above. There are some simplification of the structure details around the pontoon-column connection areas, with some stiffeners and brackets omitted, and thus the results of global model shows that the fatigue life is lower than 20 years.

The stochastic fatigue analysis is repeated by using sub-model principle and with brackets and stiffeners modelled as mentioned in Section 8.1, the results are then checked. **Figure 39** shows the fatigue usage factor of the sub-model. Noticed that the whole sub-model is with very low usage factor except that for critical such as the connection between pontoon/column, the usage factor is close to 0.4. **Figure 40** shows the expected fatigue life for the sub-model. Noticed that all locations are with fatigue life of at least 20 years above. As the design life is only 20 years, thus the structure is with fatigue design factor >10 except the connection point and a few other locations.

9 EFFECTS OF SPONSONS

9.1 Introduction

Modification works are performed on semi-submersibles for various reasons. Old drilling semi-submersibles may be converted to floating production or accommodation platforms by removing the drilling equipment installed and replacing all equipment with heavy modules used for in-situ processing, production or accommodation purpose. Prefabricated columns, additional sponsons or blisters in form of pontoon extension or others are added to the existing hull. Older generation semi-submersibles using mooring for positioning are upgraded to more advanced dynamic position semi-submersibles through major modification which usually involves the installation of thrusters and the adding of sponsons in order to increase buoyancy to compensate for the additional weight added.

For example, a 6-column twin pontoon semi-submersible is added two extra columns on the newly added pontoon extension, as shown in **Figure 41**. The thrusters are located in the extended part of pontoons and the newly added columns provide access to the thruster for maintenance purpose. Top of columns provide additional deck areas that can be used for accommodation or material storage **[30]**. Another example is the rig Homer Ferrington, **Figure 42** shows the rig before and after conversion. The conversion is performed to increase the water depth capability of the vessel so that it can be operated in deeper water depth. The conversion includes pontoon and main deck extension, the adding of new columns and sponsons.

In contrast to the major conversion that usually involves the adding of columns and pontoon extension, in some minor cases, usually only sponsons or blisters are added to a semi-submersible in order to increase its buoyancy so that its floating draft can be reduced or be able to carry more payload at the same maximum draft. Rarely but sometimes sponsons are added to a new semi-submersible building project halfway during the construction phase due to the major changes in arrangement that results in sudden increase of weight. It is possible that the weight increase is only detected after inclination test has been performed and the installation of sponsons and blisters is required before shipyard delivery. **[33]**

For semi-submersibles equipped with thrusters, if sponsons must be added during construction phase, the locations, dimensions and shapes of the sponsons must be carefully selected to minimize the impact of additional drag incurred by the additional sponsons to the overall forward speed of the unit. There are many possible types of sponson but very usually the sponsons added are always symmetric in order to minimize the change of transverse and longitudinal center of gravity.

The reference model used in previous analyses is with a total of 4 sponsons added on the unit. Each sponson is added to one of the columns to minimize the possible impact on transverse and longitudinal vertical center of gravity. The sponson is 4.5m width and starts at the height of about 2.5m below pontoon top and all the way to deck box. The total water plane area of the sponsons at any height higher than the pontoon top is almost constant and therefore when the vessel is in operating draft or survival draft the waterplane area of the sponsons are the same. The only exception is in transit draft, as the sponsons are located higher than the transit draft, no additional buoyancy contributed by the sponsons. However, it is acceptable considering the semisubmersible is a fixed semi-submersible with low mobility and the unit needs not to be in transit draft often during the entire working life of the unit.

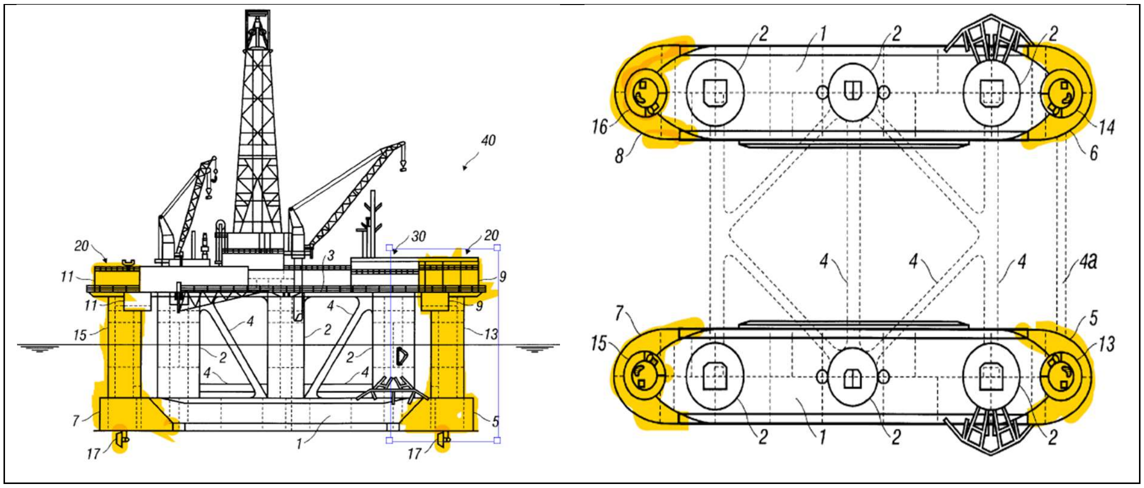

Figure 41 Conversion of semi-submersible into dynamic positioning **[30]**

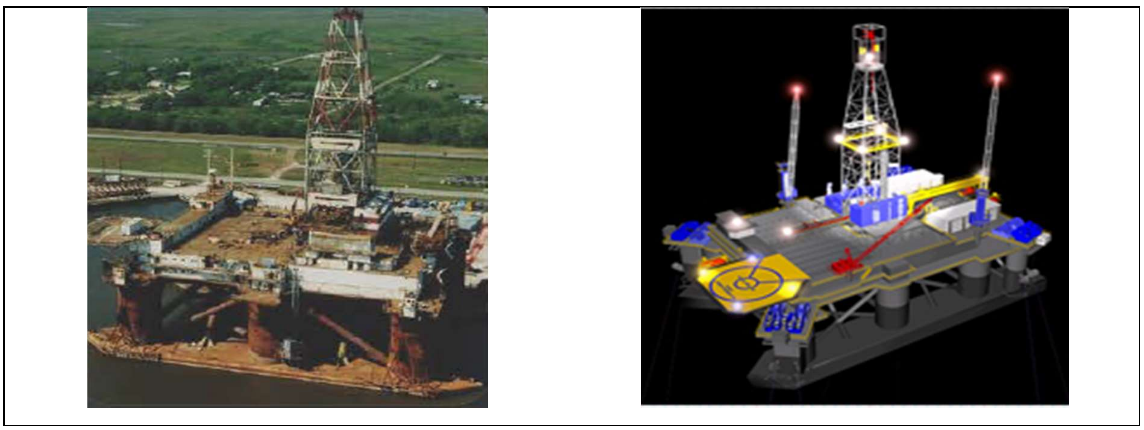

Figure 42 Conversion of Homer Ferrington, before and after **[31] [32]**

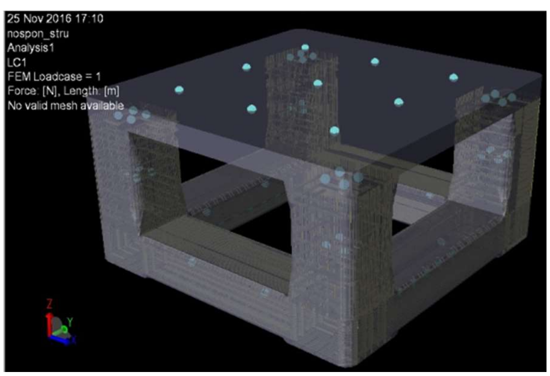

Figure 43 Structural Model without sponsons

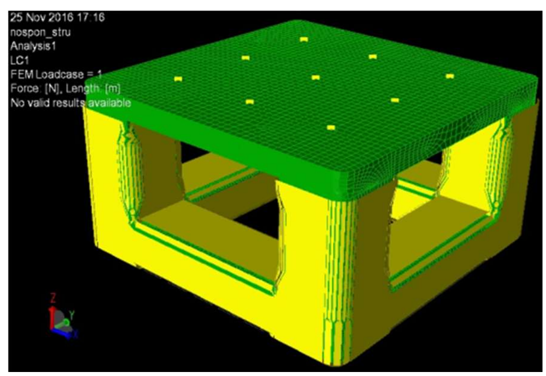

Figure 44 FE model with wetted surface

There is a total of three watertight decks at 12m, 24.5m and 33.5m from baseline respectively and there are also vertical bulkheads that break the whole sponsons into smaller compartments so that the impact due to the damage of any of them on the overall stability is minimized.

The difference between the additional weight of sponson and the buoyancye generated is the extra payload that can be used to load extra equipment and consumables onto the rig. With the installation of piping and instruccmental equipment required by Class, it is possible to use sponsons as ballast tanks so that ballast water can be used to adjust the stability of the unit. However, the ballast water may reduce the payload that can be loaded on the unit. Therefore, the sponsons are sometimes just used as void tanks.

The modified structural model to be used in analysis is shown in **Figure 43**. Plates with thickness 25mm are used for the whole structure of this model. **Figure 44** shows the FE model of the ring pontoon semi-submersible without sponsons. The yellow surfaces shown in the figure is the wet surfaces considered in hydroD analysis. Noticed that with the removal of sponsons, all side shells of columns are now covered with wetted surfaces.

9.2 Motion analyses

Motion analyses are performed for the semi-submersible without sponsons to see whether there are any differences in the motions of the vessel. The analyses are conducted using the same software and methodology discussed in Section 6 but the panel model is rebuilt by removing the sponsons attached to the columns. The existing point masses are reduced so that the draft is adjusted to a level which is almost similar to the draft used in previous motion analysis for unit with sponsons.

As the vessel is symmetrical in X and Y direction so only two wave directions are considered when comparing the motion response. Heave, pitch and roll of the unit without sponson are obtained and compared to the results obtained in Section 6.3.1. Based on **Figure 45** and **Figure 46** below, noticed that the heave motion is somehow lower (1.35m) and the peak is shifted a few seconds higher when there are no sponsons attached to the columns. The results is logical as based on the Equation **(5-1)**, when the waterplane area is reduced the heave period is increased. The same trend is observed in both directions of 0° and 45°. If the amplitude at each wave period considered in the analyses are compared, noticed that, the semi-submersible without sponsons has higher amplitude except for the period of 23s. In other words, the adding of sponsons increases the heave motion when the wave period is close to the natural period of but for those wave periods lower or higher than the natural periods, the heave motions are lesser. As a semi-submersible is always designed with natural period higher than the prevalent wave period so the adding of sponsons is considered acceptable as there is only a slight increase. **Table 16** shows the comparison result of heave motion at different wave period.

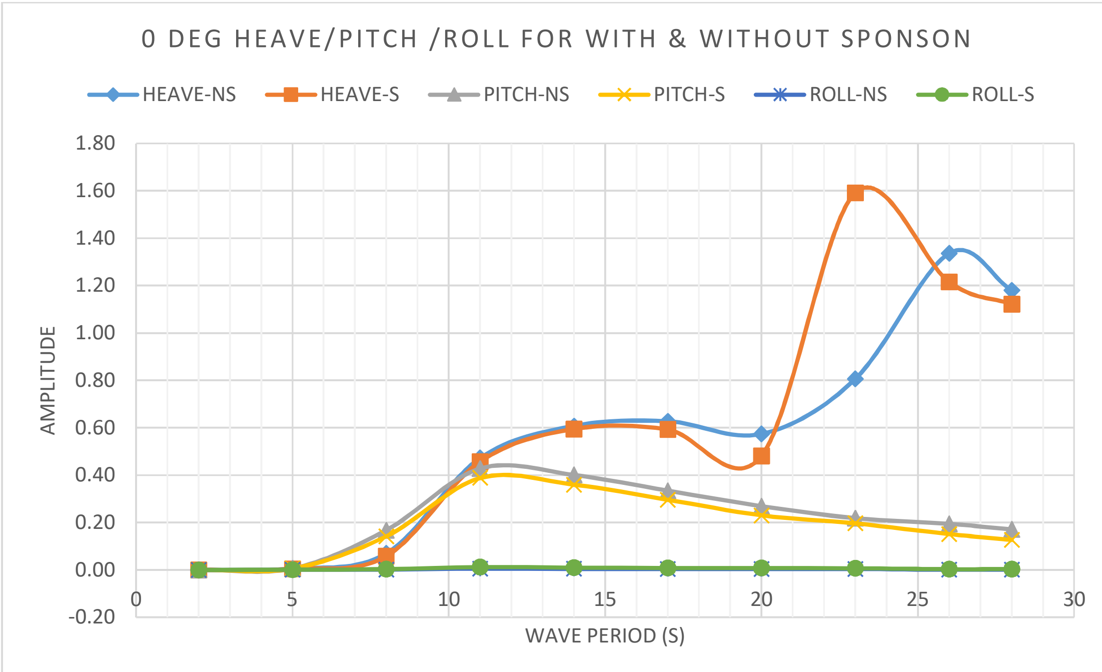

Figure 45 RAO at 0 degree (S=with sponsons, NS=without sponsons)

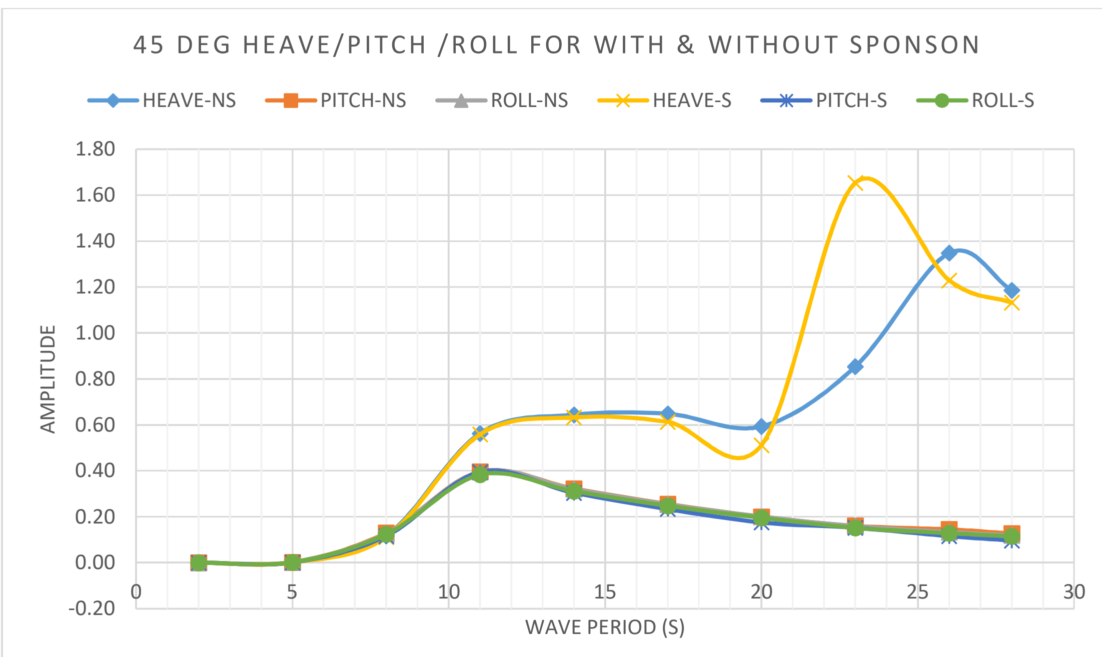

Figure 46 RAO at 45 degree (S=with sponsons, NS=without sponsons)

A look on the comparison of roll and pitch in **Figure 45** and **Figure 46**, noticed that the trends are almost similar for both with and without sponsons at 0° and 45° direction. The motion responses are not as serious as heave response and also the differences are not too much. Therefore, the adding of sponsons actually brings less impact for roll and pitch. For the comparison results of roll and pitch motions at different wave period, refer Appendices Section 15.3.

Table 16 Comparison result for heave motion

Period	Heave at 0 degree		Diff	Heave at 45 degree		Diff
s	Sponson	NoSponson	%	Sponson	NoSponson	%
28	1.12E+00	1.18E+00	5%	1.13E+00	1.19E+00	5%
26	1.22E+00	1.34E+00	10%	1.23E+00	1.35E+00	10%
23	1.59E+00	8.06E-01	-49%	1.65E+00	8.54E-01	-48%
20	4.81E-01	5.74E-01	19%	5.12E-01	5.93E-01	16%
17	5.93E-01	6.27E-01	6%	6.13E-01	6.48E-01	6%
14	5.95E-01	6.07E-01	2%	6.33E-01	6.44E-01	2%
11	4.57E-01	4.72E-01	3%	5.59E-01	5.64E-01	1%
8	5.79E-02	6.91E-02	19%	1.11E-01	1.17E-01	6%
5	4.64E-03	5.30E-03	14%	2.03E-03	2.68E-03	32%
2	9.39E-06	3.80E-05	304%	8.60E-06	8.22E-06	-4%

9.3 Hydrodynamic Analysis

The same analysis set up and methodology used in Section 6.3.2 are reused here. The distribution of hydrodynamic load on the semi-sumersible without sponsons is studied under the same set of load cases. The load factor for permanent & variable functional loads, for combination-a, is taken as 1.3 as well. The combination of all load cases is shown in **Figure 47** and by taking into consideration the permanent & variable functional loads, the ULS combination-a is shown in **Figure 48**. Noticed from these two figures that the critical areas with higher stress concentration such as pontoon-column connection points are almost similar with the results obtained from hull shape with sponsons in Section 6.3.2. With these, the adding of sponsons actually bring no tremendous changes to the overall global structural strength as the sides of columns where the sponsons attached to are not areas with high stress concentration.

Table 17 shows the summary of the von Mises stress on each part of the unit based on load combination-a. As mentioned in Section 9.1, the plate thickness of the model without sponsons are set to 25mm whereas for the model with sponsons, most of the plate thickness are less than 25mm except for the a very small portion located at the connection points between pontoons and columns, as shown in **Figure 22**. Therefore, among other factors, the von Mises stress in **Table 17** is generally lower as compared to the results in **Table 10**.

Table 17 Summary of Von Mises stress distribution

No	Location	Stress Range (N/mm^2)
1	Pontoon Top Plate	< 125
2	Pontoon Bottom Plate	<150
3	Pontoon vertical side shell near columns	< 150
4	Pontoon-Column connection point	<260
5	Column side shell facing inwards	<180
6	Column side shell facing outwards	< 80
7	Sponson	-

9.4 Fatigue Analysis

Stochastic fatigue analysis is performed on global model to check the possible differences between unit with and without sponsons. The Stofat setup is as per mentioned in Section 8.3. The results are shown in **Figure 49** and **Figure 50**. Noticed from these two figures that, the spots vulnerable to fatigue damage are not much different from the results shown in Section 8.3 even after the removal of sponsons, with critical areas still on the pontoon-column connetion facing inwards and on the side shells that facing outboard.

On the critical areas, an extra check on the hotspot stress is performed to estimate the fatigue life of welds. From the semi-submersible without sponsons, the stiffened plate located at the center of the pontoon-column connection is selected, as shown in **Figure 51**. A sub-model of the stiffened plate is prepared and FE model with mesh size of 1cm x 1cm is generated, as shown in **Figure 52**. The total element for the submodel is 61058 elements. The lower part of the stiffened plate is with plate thickness of 25mm and the stiffener is bulb flat with dimension 280*12t. And thus, the mesh element used is about 0.4* plate thickness. Fatigue analysis is then performed using Sub-model principle and similar stofat setup mentioned in Section 8. The misalignment and geometrical stress concentration factor is set to 1.0. Only lower part of the stiffened plate is considered in Stofat, as highlighted in **Figure 52**.

The fatigue usage factor of the stiffened plate is shown in **Figure 53**. Noticed that there is an element with higher usage factor at the bottom of the sub-model. As the top plate of pontoon is not modelled and this element is located on the boundary area of sub-model, the value given by the boundary elements should not be considered. Other elements located some distances away from boundaries (in Z direction) show lower usage factor. A check on maximun stress shows that, the long term maximun stress of 100-year is low, as shown in **Figure 54**. With these results, the minimun fatigue design life of 20 years is fulfilled and the fatigue design factor is at least >10.

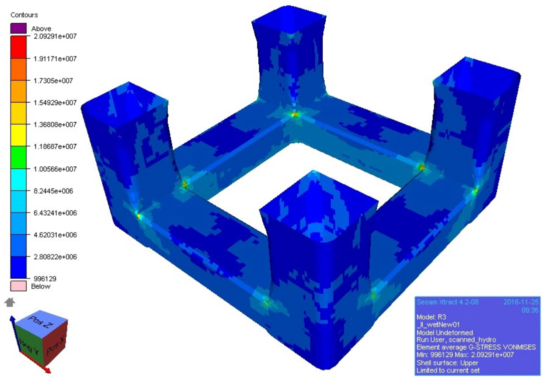

Figure 47 Combination of all load cases

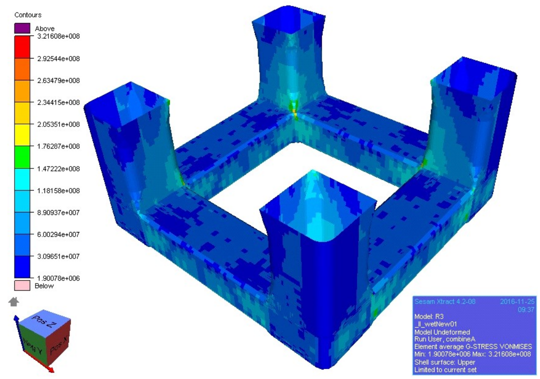

Figure 48 ULS Combination a

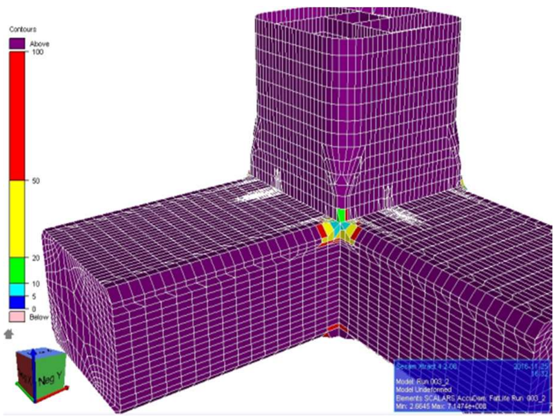

Figure 49 Fatigue life01 (Global Model – no sponsons)

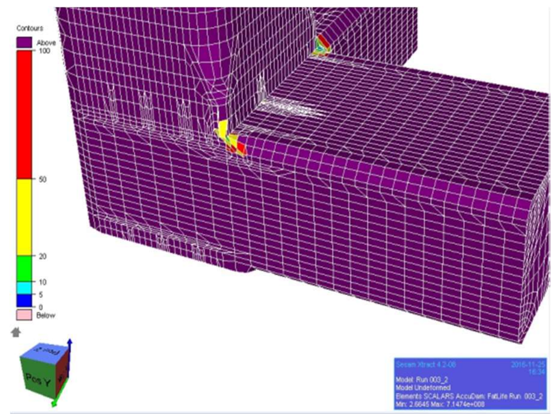

Figure 50 Fatigue life02 (Global Model – no sponsons)

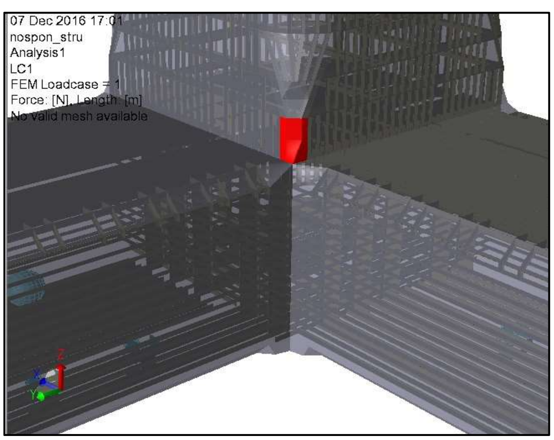

Figure 51 Stiffened plate (centre) for fatigue analysis

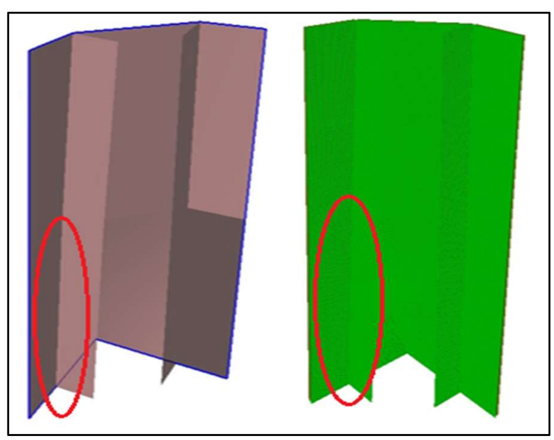

Figure 52 Structure and FE models (centre)

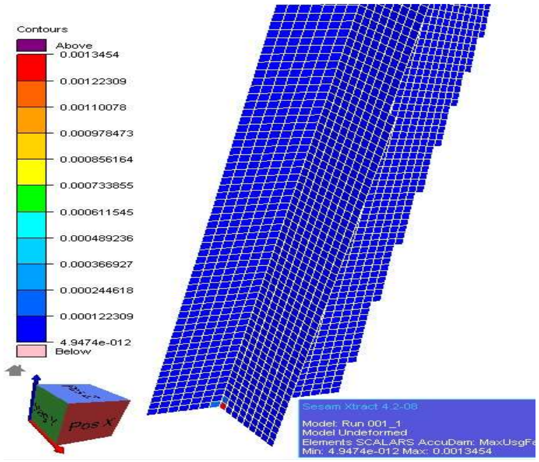

Figure 53 Stiffened plate (centre) - Fatigue usage factor

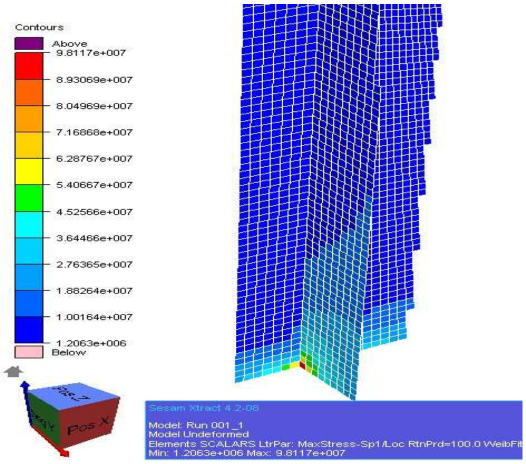

Figure 54 Stiffened plate (centre) – 100-year max principal stress

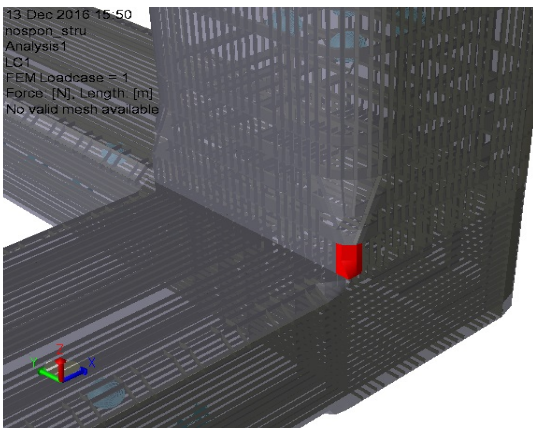

Figure 55 Stiffened plate (side) for fatigue analysis

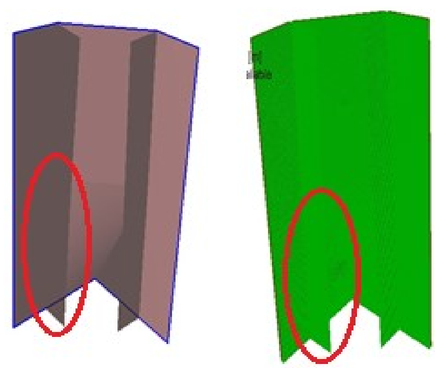

Figure 56 Structure and FE models (side)

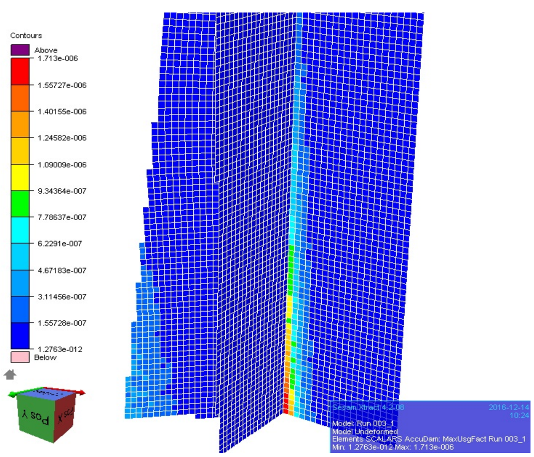

Figure 57 Stiffened plate (Side) - Fatigue usage factor

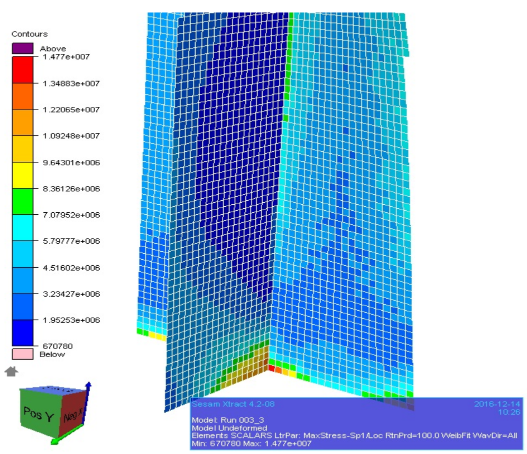

Figure 58 Stiffened plate (Side) – 100-year max principal stress

The same fatigue analysis is repeated on the stiffened plate located at the side shell of the semi-submersible, as highlighted in **Figure 55**. Similarly, only lower part of the stiffened plate is considered in Stofat, as highlighted in **Figure 56**. The fatigue usage factor is shown in **Figure 57** and the 100-year maximum principal stress is shown in **Figure 58**. Noticed that the stiffened plate (side) is with design life higher than the fatigue design life but less critical in comparison to the stiffened plate (center) because of the lower fatigue usage factor and maximum principal stress.

9.5 Summary

By removing the sponsons attached to the four columns, analyses are performed and the impacts are studied. For motion responses, there are minor differences except in term of heave. The heave responses is higher and the peak period is lower when there is the addition of sponsons. Based on the results of hydrodynamic and fatigue analyses of global models, the results for semi-submersible with and without sponsons show that the stress concentration areas are almost the same and the adding of sponsons on columns bring no big impact.

As the main focus here is on the external hull of the semi-submersible, therefore only two structural panels considered to be critical from global analyses are analyzed further. In fact, for the actual case, the whole unit including internal parts which consists of many openings, penetrations and all kinds of complicated structural details should be scanned in fatigue analyses for critical areas. And then, fatigue analyses are conducted using the models of stiffened panels with complete structural details of the respective areas in sufficient mesh size to estimate the respective fatigue life.

Other than the method involving four sponsons mentioned above, there are also some other methods to increase the operational draft of a semi-submersible and generate more buoyancy. For example, extending the pontoons and adding extra columns, as shown in Figure 41. Methods adopted depend on various factors for example, the time and cost involved, available facilities and also owners' preference. Analyses performed here are only to compare the possible impact of sponsons in a quick way, more detailed structural and hydrodynamic studies should be performed taking into consideration such as the actual site operational requirement from operators, classification societies and others. Optimization on sponsons by modifying the shape and adjusting the dimensions should be performed to improve the global response of a semi-submersible.

10 CONCLUSIONS

In this thesis, fatigue analyses on ring pontoon semi-submersibles are carried out. The FE models consists of panel model, Morison model, structural and mass model are prepared based on the reference drawings provided. The models are then used as inputs for global responses and hydrodynamic analyses. From the global responses analyses, the maximum heave is found to be about 1.6 and the period is about 23 second, quite similar to the calculation based on the formulas given in rules. Other responses such as surge, sway and yaw are comparatively small.

For the hydrodynamic analyses, appropriate load cases are selected based on the characteristic global responses which are governing for the global strength of a semi-submersible. The results obtained are then processed using the partial load factors of ULS to find the maximum von Mises stress acting on the structure. Based on the stress results, the critical areas such as the pontoon-column connection points are identified. Quick screen fatigue check is then performed to estimate the allowable stress range for the required design life of 20 years, based on the charts and tables given in DNVGL-RP-C203. By comparing the allowable stress range and the von Mises stresses obtained from previous hydrodynamic analyses. Most of the structures are with von Mises stresses lesser than the allowable stress range except for a few critical areas such as the pontoon-column connection points.

Stochastic fatigue analyses are repeated a few times by using FE models with different sizes of mesh ranging from global model with mesh 2m x 2m, sub-model with mesh of 0.1m x 0.1m to stiffened plate with mesh 0.01m x 0.01m. The results from global model fatigue analyses show that only the fatigue design life of pontoon-column connection point facing inwards and facing outwards (on side shells) are with fatigue design life lesser than 20 years. Results from the repeated analyses using sub-model, with finer meshes and the structural details like brackets and stiffeners fully modelled, show that the fatigue design life for the pontoon-column connection points is actually sufficient to meet the design life required. However, as mentioned in Section 9.5, the whole unit of semi-submersible must be scanned to find out the fatigue critical areas. For areas with fatigue design life lesser than the required, there are some methods to improve the fatigue life and the practicability of each method is very much depending on the stage of construction.

During the design stage, structural details may be refined and optimized to avoid stress concentration by adding reinforcement in forms of brackets and stiffeners or modifying the shape of the load-bearing structure for smoother load transition and better stress continuity. Furthermore, welds limit the load-bearing strength of a structural detail if the welds are located on the high-stressed spots such as the corners of opening and not properly prepared based on design codes. TIG dressing or some other fatigue life improvement methods aforementioned may be used to extend the fatigue life. In case the structural details are complicated, welds can be shifted away from high-stressed spots by replacing the welded panels with an one-piece casting. For this thesis, the pontoon-column connection analysed above might be replaced with cast integral to reduce the complex stress concentration and fatigue damage.

Global responses, hydrodynamic and fatigue analyses mentioned are repeated using the same semi-submersible without sponsons attached to the columns. Noticed that the heave responses are higher and the peak period is lower whereas other responses are almost the same. For global hydrodynamic and fatigue analysis, the stress distribution and concentration areas are almost the same too. Fatigue analyses are performed on two structural panel located on the pontoon-column connection point at the center and side of the semi-submersible by using FE model with mesh size of 1cm x 1cm. Both long term maximum stress of 100-year and usage factor are low. Therefore, based on the assumptions and the loading condition considered, the adding of sponsons brings minor impact on the semi-submersible in terms of global responses, hydrodynamic load and fatigue life. However, more thorough hydrodynamic and fatigue analyses taking into consideration the actual environmental conditions and possible changes of loading conditions must be done to verify the results.

11 FUTURE WORKS & RECOMMENDATIONS

Ballast and mooring loads - Analyses above are performed without applying the loads of ballast and other types of liquids in the tanks. The weight of ballast and the liquids are simplified and replaced with point masses. The impact of ballast loads on the global and local structure in term of strength and fatigue may be considered if the point masses are replaced with liquids when the analyses is performed in HydroD. Similar to ballast loads, mooring loads may be applied on the vessels if the information on mooring loads and mooring arrangement such as the exact locations of mooring winches, fairleads and others are available.

Wave period and directional probability - Regular wave periods used in the analyses are ranging from 2s to 28s and with constant 3s gap. More wave periods with smaller gap may be used to find more accurate results especially for the wave periods that is close to the natural period of the structure so that the maximum global response can be accurately captured. However, the selection of too many and unnecessary wave periods may make the analysis process more time consuming. Careful selection of wave period is important after considering the pros and cons. In addition, for the water directional probability considered in stochastic fatigue analysis, it is assumed that possibility of wave coming from each direction is the same. For a site specific offshore structure, actual wave directional probability, together with site wave scatter diagrams, should be used to obtain better results.

Structural model – For analyses performed above, a typical compartmentation and structure arrangement is applied for all four columns and some structural details such as openings, penetrations reinforcement, insert plates, brackets and others are ignored or simplified. In future, for better estimation of the fatigue life, structures located close to stress concentration area should be modelled as detailed as possible. For critical areas, mesh size similar or less then the thickness of plate concerned must be used to calculate the hotspot stresses and corresponding fatigue damage.

12 DECLARATION OF AUTHORSHIP

I declare that this thesis and the work presented in it are my own and have been generated by me as the result of my own original research.

Where I have consulted the published work of others, this is always clearly attributed.

Where I have quoted from the work of others, the source is always given. With the exception of such quotations, this thesis is entirely my own work.

I have acknowledged all main sources of help.

Where the thesis is based on work done by myself jointly with others, I have made clear exactly what was done by others and what I have contributed myself.

This thesis contains no material that has been submitted previously, in whole or in part, for the award of any other academic degree or diploma.

I cede copyright of the thesis in favour of the Pomeranian University of Technology, Szczecin

Date: *Signature*

13 ACKNOWLEDGEMENTS

I would like to thank Professor Maciej Taczala from Zachodniopomorski Uniwersytet Technologiczny w Szczecinie (ZUT) as my master thesis supervisor and Mr. Tomasz Msciwujewski, the head of the section of Advisory Maritime and Offshore, DNV-GL Gdynia, Poland for their coordination to make both the thesis and internship possible. Furthermore, Mr. Maciej Jasinski , Mr. Piotr Dolebski, Mr. Sebastian Tocha and many more colleagues who are ready to help and provide guidance during my internship in DNV-GL Gdynia.

Also, I would like to thank all coursemates and professors from University de Liege (ULg); Ecole Centrale de Nantes (ECN) and ZUT that have helped me very much during my 18 months study.

This thesis was developed in the frame of the European Master Course in "Integrated Advanced Ship Design" named "EMSHIP" for "European Education in Advanced Ship Design", Ref.: 159652-1-2009-1-BE-ERA MUNDUS-EMMC.

14 REFERENCES

[1] KeppelCorp, 30 May 2005. [Online]. Available: http://www.kepcorp.com/en/news_item.aspx?sid=1008.

[2] PrinciplePower. [Online]. Available: http://www.principlepowerinc.com/fileManager/editor/pdfs/PrinciplePowerWindFloatBrochure.pdf.

[3] M. K. (. a. C. M. (NTNU), "Dynamic Analysis of a Braceless Semisubmersible Offshore Wind Turbine in Operational Conditions".

[4] J. Halkyard, Design and Analysis of Floating Structures, Houston, Texas USA: John Halkyard & Associates, 2013.

[5] DNV, RP-C203 Fatigue Design of Offshore Steel Structure, DNV, Apr 2010.

[6] A. Hobbacher, Reccommendations for Fatigue Design of Welded Joints and Components, International Institue of Welding, Dec 2008.

[7] "Fatigue design based on S-N Data," [Online]. Available: http://homes.civil.aau.dk/lda/Advanced%20Structural%20Engineering/Fatigue%20design%20based%20on%20S-N%20data.pdf. [Accessed 19 11 2016].

[8] DNV, CN 30.7 Fatigue Assessment of Ship Structures, DNV, Apr 2014.

[9] M. M. e. a. Pedersen, "Experience with the Notch Stress Approach for Fatigue Assessment of Welded Joints," in *Proceedings of Swedish Conference on Lightweight Optimised Welded Structures*.

[10] D. o. C. E. T. I. o. Technology., "Nominal Stress Based. Fatigue Design," [Online].
_ Available: http://www.ocw.titech.ac.jp/index.php?module=General&action=DownLoad&file=20092224611005-17-0-9.pdf&type=cal&JWC=20092224611005. [Accessed 19 11 2016].

[11] ABS, Guide for Fatigue Assessment of Offshore Structures, ABS, Feb 2014.

[12] "Weld Detail Fatigue Life Improvement Techniques," [Online]. Available: http://www.shipstructure.org/pdf/400.pdf. [Accessed 19 11 2016].

[13] ABS, Guide for Spectral-Based Fatigue Analysis for Floating Production, Storage and Offloading (FPSO) Installations, May 2010.

[14] DNV, RP-C206 Fatigue Methodology of Offshore Ships, DNV, Oct 2012.

[15] “Improvement Techniques in Welded Joints,” [Online]. Available: http://fgg-web.fgg.uni-lj.si/~/pmoze/esdep/master/wg12/l0500.htm. [Accessed 19 11 2016].

[16] DNV-GL, “SE13- Sesam User Course Material”.

[17] DNV, “DNV-RP-H103 Modelling and Analysis of Marine Operations,” April 2011.

[18] DNV, “RP-C205 Environmental Conditions and Environmental Loads,” April 14.

[19] DNV-GL, “DNVGL-OS-C101 Design of offshore steel structures, general - LRFD Method,” April 16.

[20] DNV-GL, “DNVGL-RP-C103. Column-Stabilised Units,” July 15.

[21] ABS, “Guidance Notes on Global Performance Analysis for Floating Offshore Wind Turbine Installation,” Feb 14.

[22] DNV, “DNV-RP-F205 Global Performance Analysis of Deep Water Flaoting Structure,” Oct 10.

[23] L. Borgman, “Directional spectra models for design use,” in *Proceedings of Offshore Technology Conference Paper OTC 1069*, 1969.

[24] G. Ducrozet, Water Waves and Sea State Models for Ship Design (Lecture Notes).

[25] DNV, Sesam User Manual - STOFAT, April 11.

[26] DNV-GL, “Structural design of column stabilised units - LRFD method,” July 15.

[27] Norsok, “N-001 Structural Design,” Feb 2004.

[28] C. C. Society, “No.56 Fatigue Assessment of Ship Structure,” 1999.

[29] Wikipedia, “Fatigue (material),” [Online]. Available: https://en.wikipedia.org/wiki/Fatigue_(material)#Stress-cycle_.28S-N.29_curve. [Accessed 2016 11 19].

[30] “Patent US 6247421 B1 Method for DP-conversion of an existing semi-submersible rig,” [Online]. Available: https://www.google.com/patents/US6247421. [Accessed 19 11 2016].

[31] “Zentech Company Presentation,” [Online]. Available: http://zentech-usa.com/wp-content/uploads/2014/09/Zentech-Company-Presentation-5-2015-Web.pdf. [Accessed 19 11 2016].

[32] “Stafford Conversion,” [Online]. Available: http://www.stafford-design.com/tplstd.asp?page=330. [Accessed 19 11 2016].

[33] “Songa Semi Conversion,” [Online]. Available: http://www.marinelog.com/index.php?option=com_k2&view=item&id=8911:newbuild-songa-semi-to-get-sponsons-and-blisters&Itemid=231. [Accessed 19 11 2016].

[34] DNV, Fatigue Assessment Using SESAM Program Modules Stofat, Framework and Postresp, DNV.

[35] DNV, Sesam User Manual, DNV, Jan 2010.

[36] M. Aygul, Fatigue Analysis of Welded Structures Using the Finite Element Method, Gothenburg, Sweden: Chalmers University of Technology, 2012.

15 APPENDICES

15.1 DNA-NA Wave Scatter Diagram

*Generated using DNV Sesam STOFAT and tabulated using Excel

Name: DNV-NA
Decription: DNV North Atlantic

Hs	Tz	Prob
1.0	4.5	7.20E-04
2.0	4.5	5.00E-05
1.0	5.5	1.42E-02
2.0	5.5	3.65E-03
3.0	5.5	6.20E-04
4.0	5.5	1.20E-04
5.0	5.5	2.00E-05
6.0	5.5	1.00E-05
1.0	6.5	4.59E-02
2.0	6.5	3.30E-02
3.0	6.5	1.08E-02
4.0	6.5	3.18E-03
5.0	6.5	8.90E-04
6.0	6.5	2.50E-04
7.0	6.5	7.00E-05
8.0	6.5	2.00E-05

Hs	Tz	Prob
9.0	6.5	1.00E-05
1.0	7.5	4.94E-02
2.0	7.5	8.00E-02
3.0	7.5	4.43E-02
4.0	7.5	1.90E-02
5.0	7.5	7.21E-03
6.0	7.5	2.54E-03
7.0	7.5	8.50E-04
8.0	7.5	2.70E-04
9.0	7.5	8.00E-05
10.0	7.5	3.00E-05
11.0	7.5	1.00E-05
1.0	8.5	2.59E-02
2.0	8.5	8.02E-02
3.0	8.5	6.92E-02
4.0	8.5	4.13E-02
5.0	8.5	2.04E-02
6.0	8.5	8.96E-03
7.00	8.5	3.63E-03
8.00	8.5	1.38E-03
9.00	8.5	5.00E-04

Hs	Tz	Prob
10.0	8.5	1.70E-04
11.0	8.5	6.00E-05
12.0	8.5	2.00E-05
13.0	8.5	1.00E-05
1.0	9.5	8.39E-03
2.0	9.5	4.39E-02
3.0	9.5	5.57E-02
4.0	9.5	4.44E-02
5.0	9.5	2.77E-02
6.0	9.5	1.48E-02
7.0	9.5	7.09E-03
8.0	9.5	3.12E-03
9.0	9.5	1.28E-03
10.0	9.5	5.00E-04
11.0	9.5	1.80E-04
12.0	9.5	7.00E-05
13.0	9.5	2.00E-05
14.0	9.5	1.00E-05
1.00	10.5	1.95E-03
2.00	10.5	1.57E-02
3.00	10.5	2.79E-02

Hs	Tz	Prob
4.00	10.5	2.89E-02
5.00	10.5	2.23E-02
6.00	10.5	1.42E-02
7.00	10.5	7.91E-03
8.00	10.5	3.98E-03
9.00	10.5	1.84E-03
10.00	10.5	8.00E-04
11.00	10.5	3.30E-04
12.00	10.5	1.30E-04
13.00	10.5	5.00E-05
14.00	10.5	2.00E-05
15.00	10.5	1.00E-05
1.00	11.5	3.60E-04
2.00	11.5	4.14E-03
3.00	11.5	9.93E-03
4.00	11.5	1.30E-02
5.00	11.5	1.21E-02
6.00	11.5	9.07E-03
7.00	11.5	5.80E-03
8.00	11.5	3.30E-03
9.00	11.5	1.71E-03

Hs	Tz	Prob
10.0	11.5	8.20E-04
11.0	11.5	3.70E-04
12.0	11.5	1.50E-04
13.0	11.5	6.00E-05
14.00	11.5	2.00E-05
15.00	11.5	1.00E-05
1.00	12.5	5.00E-05
2.0	12.5	8.70E-04
3.0	12.5	2.74E-03
4.0	12.5	4.45E-03
5.0	12.5	4.94E-03
6.00	12.5	4.28E-03
7.00	12.5	3.11E-03
8.00	12.5	1.97E-03
9.0	12.5	1.13E-03
10.0	12.5	5.90E-04
11.0	12.5	2.90E-04
12.0	12.5	1.30E-04
13.00	12.5	6.00E-05
14.00	12.5	2.00E-05
15.00	12.5	1.00E-05

Hs	Tz	Prob
16.0	12.5	1.00E-05
1.0	13.5	1.00E-05
2.0	13.5	1.60E-04
3.0	13.5	6.30E-04
4.00	13.5	1.24E-03
5.00	13.5	1.62E-03
6.00	13.5	1.60E-03
7.0	13.5	1.31E-03
8.0	13.5	9.20E-04
9.0	13.5	5.80E-04
10.0	13.5	3.30E-04
11.00	13.5	1.70E-04
12.00	13.5	8.00E-05
13.00	13.5	4.00E-05
14.0	13.5	2.00E-05
15.0	13.5	1.00E-05
2.0	14.5	3.00E-05
3.0	14.5	1.20E-04
4.00	14.5	3.00E-04
5.00	14.5	4.50E-04
6.00	14.5	5.00E-04

Hs	Tz	Prob
7.0	14.5	4.60E-04
8.0	14.5	3.50E-04
9.0	14.5	2.40E-04
10.0	14.5	1.50E-04
11.00	14.5	8.00E-05
12.00	14.5	4.00E-05
13.00	14.5	2.00E-05
14.0	14.5	1.00E-05
3.0	15.5	2.00E-05
4.0	15.5	6.00E-05
5.0	15.5	1.10E-04
6.00	15.5	1.40E-04
7.00	15.5	1.40E-04
8.00	15.5	1.20E-04
9.0	15.5	9.00E-05
10.0	15.5	6.00E-05
11.0	15.5	3.00E-05
12.0	15.5	2.00E-05
13.00	15.5	1.00E-05
14.00	15.5	1.00E-05
4.00	16.5	1.00E-05

Hs	Tz	Prob
5.0	16.5	2.00E-05
6.0	16.5	3.00E-05
7.0	16.5	4.00E-05
8.0	16.5	3.00E-05
9.00	16.5	3.00E-05
10.00	16.5	2.00E-05
11.00	16.5	1.00E-05
12.0	16.5	1.00E-05
5.0	17.5	1.00E-05
6.0	17.5	1.00E-05
7.0	17.5	1.00E-05
8.00	17.5	1.00E-05
9.00	17.5	1.00E-05
10.00	17.5	1.00E-05

Total probability: 1.0
Number of statistics points: 156

15.2 Stofat Input File

```
%----------------------------------------
% Read .SIN file and transfer superelement
%---------------------------------------
%
% Create wave statistics
%----------------------
%
CREATE WAVE-SPREADING-FUNCTION COS4 Continuous COSINE-POWER 4
%
% Assign wave data
%-----------------
ASSIGN WAVE-SPREADING-FUNCTION DNV-NA COS10 ALL
ASSIGN WAVE-SPECTRUM-SHAPE DNV-NA PIERSON-MOSKOWITZ ALL
ASSIGN WAVE-DIRECTION-PROBABILITY 0.0 0.125
ASSIGN WAVE-DIRECTION-PROBABILITY 45.0 0.125
ASSIGN WAVE-DIRECTION-PROBABILITY 90.0 0.125
ASSIGN WAVE-DIRECTION-PROBABILITY 135.0 0.125
ASSIGN WAVE-DIRECTION-PROBABILITY 180.0 0.125
ASSIGN WAVE-DIRECTION-PROBABILITY 225.0 0.125
ASSIGN WAVE-DIRECTION-PROBABILITY 270.0 0.125
ASSIGN WAVE-DIRECTION-PROBABILITY 315.0 0.125
ASSIGN WAVE-STATISTICS 0.0 DNV-NA
ASSIGN WAVE-STATISTICS 45.0 DNV-NA
ASSIGN WAVE-STATISTICS 90.0 DNV-NA
ASSIGN WAVE-STATISTICS 135.0 DNV-NA
ASSIGN WAVE-STATISTICS 180.0 DNV-NA
ASSIGN WAVE-STATISTICS 225.0 DNV-NA
ASSIGN WAVE-STATISTICS 270.0 DNV-NA
ASSIGN WAVE-STATISTICS 315.0 DNV-NA
%
%
SELECT SET ELEMENTS Current INCLUDE ALL
%
%
ASSIGN SN-CURVE Current DNV2010_F-SEAFC
ASSIGN K-FACTORS Current 1.0 1.0 1.0 1.0 1.0
%
```

15.3 Comparison Result (Roll and Pitch)

Follwoing tables show the comparison result between semi-surmersibles with and without sponson in terms of Roll and Pitch (at wave direction of 0 and 45 degress)

Period	Roll at 0 degree		Diff	Roll at 45 degree		Diff
s	Sponson	NoSponson	%	Sponson	NoSponson	%
28	3.37E-03	1.14E-03	-66%	1.15E-01	1.19E-01	4%
26	2.99E-03	4.62E-04	-85%	1.29E-01	1.33E-01	4%
23	6.75E-03	3.69E-03	-45%	1.52E-01	1.60E-01	5%
20	7.91E-03	3.19E-03	-60%	1.96E-01	2.01E-01	3%
17	7.83E-03	3.38E-03	-57%	2.48E-01	2.55E-01	3%
14	9.54E-03	4.16E-03	-56%	3.12E-01	3.21E-01	3%
11	1.17E-02	5.20E-03	-56%	3.83E-01	3.96E-01	3%
8	3.01E-03	1.33E-03	-56%	1.24E-01	1.27E-01	3%
5	7.71E-04	3.72E-04	-52%	1.66E-03	2.36E-03	42%
2	2.16E-06	4.91E-06	128%	1.25E-05	7.43E-06	-41%

Period	Pitch at 0 degree		Diff	Pitch at 45 degree		Diff
s	Sponson	NoSponson	%	Sponson	NoSponson	%
28	1.27E-01	1.71E-01	35%	9.69E-02	1.27E-01	31%
26	1.51E-01	1.94E-01	28%	1.16E-01	1.45E-01	25%
23	1.96E-01	2.18E-01	11%	1.52E-01	1.61E-01	6%
20	2.30E-01	2.69E-01	17%	1.76E-01	2.00E-01	14%
17	2.96E-01	3.34E-01	13%	2.34E-01	2.56E-01	9%
14	3.60E-01	4.01E-01	11%	3.04E-01	3.22E-01	6%
11	3.88E-01	4.28E-01	10%	3.95E-01	3.96E-01	0%
8	1.42E-01	1.68E-01	18%	1.17E-01	1.30E-01	12%
5	5.44E-03	5.68E-03	4%	1.61E-03	1.54E-03	-4%
2	2.44E-05	8.09E-05	231%	9.48E-06	1.08E-05	14%

15.4 Maximun Elemets in Stofat

*Tables below are from DNV, Sesam User Manual - Stofat

Number of sea states (nsea)	Number of wave direction frequencies (nwdir*nfreq)	Data base pages to store results of one element	Maximum number of elements that may be included in a Stofat run
6143 - 6654	3070 - 3326	13	5040
5631 - 6142	2814- 3069	12	5460
5119 - 5630	2558 - 2813	11	5956
4607 - 5118	2302 - 2557	10	6553
4095 - 4606	2046 - 2301	9	7281
3583 - 4094	1790 - 2045	8	8192
3071 - 3582	1534 - 1789	7	9362
2559 - 3070	1278 - 1533	6	10922
2047 - 2558	1022 - 1277	5	13107
1535 - 2046	766 - 1021	4	16383
1023 - 1534	510 - 765	3	21845
511 - 1022	254 - 509	2	32767
255 - 510	126 - 253	1	65535
69 - 254	83 - 125	1/2	131070
127 - 168	62 - 82	1/3	191605

Number of sea states (nsea)	Number of wave direction frequencies (nwdir*nfreq)	Data base pages to store results of one element	Maximum number of elements that may be included in a Stofat run
101 - 126	49 - 61	1/4	262140
84 - 100	40 - 48	1/5	327675
72 - 83	34 - 39	1/6	393210
63 - 71	30 - 33	1/7	458745
All elements are assumed to have 8 stress points			